RSC Advances

PAPER

View Article Online
View Journal | View Issue

Cite this: *RSC Adv.*, 2020, **10**, 1552

Exploring the metabolic biomarkers and pathway changes in crucian under carbonate alkalinity exposure using high-throughput metabolomics analysis based on UPLC-ESI-QTOF-MS†

Yan-chun Sun, ‡[a] Shi-cheng Han,‡[a] Ming-zhu Yao,‡[ab] Hong-bai Liu*[a] and Yu-mei Wang *[a]

The aims of this study is to explore the metabolomic biomarker and pathway changes in crucian under carbonate alkalinity exposures using high-throughput metabolomics analysis based on ultra-performance liquid chromatography-electrospray ionization-quadrupole time of flight-tandem mass spectrometry (UPLC-ESI-QTOF-MS) for carrying out adaptive evolution of fish in environmental exposures and understanding molecular physiological mechanisms of saline–alkali tolerance in fishes. Under 60 day exposure management, the UPLC-ESI-QTOF-MS technology, coupled with a pattern recognition approach and metabolic pathway analysis, was utilized to give insight into the metabolic biomarker and pathway changes. In addition, biochemical parameters in response to carbonate alkalinity in fish were detected for chronic impairment evaluation. A total of twenty-seven endogenous metabolites were identified to distinguish the biochemical changes in fish in clean water under exposure to different concentrations of carbonate alkalinity (CA); these mainly involved amino acid synthesis and metabolism, arachidonic acid metabolism, glyoxylate and dicarboxylate metabolism, pyruvate metabolism and the citrate cycle (TCA cycle). Compared with the control group, CA exposure increased the level of blood ammonia; TP; ALB; Gln in the liver and gills; GS; urea in blood, the liver and gills; CREA; CPS; Glu and LDH; and decreased the level of weight gain rate, oxygen consumption, discharge rate of ammonia, SOD, CAT, ALT, AST and Na^+/K^+-ATPase. At low concentrations, CA can change the normal metabolism of fish in terms of changing the osmotic pressure regulation capacity, antioxidant capacity, ammonia metabolism and liver and kidney function to adapt to the CA exposure environment. As the concentration of CA increases, various metabolic processes in crucian are inhibited, causing chronic damage to the body. The results show that the metabolomic strategy is a potentially powerful tool for identifying the mechanisms in response to different environmental exposomes and offers precious information about the chronic response of fish to CA.

Received 6th October 2019
Accepted 6th December 2019

DOI: 10.1039/c9ra08090b

rsc.li/rsc-advances

1. Introduction

It is generally believed that fish in the natural world will face a certain degree of exposure to harm due to changes in environmental conditions, which lead to fish presenting stress resistance or chronic injury, even death.[1,2] Salinity and alkalinity are inseparable from the toxic effects on aquatic animals.[3] Studies have demonstrated that fish have to consume a large quantity of energy under salinity and alkalinity stress.[4] When organic matter is decomposed and energized, a large amount of O^{2-}, OH^- and other free radicals are generated. The free radicals in the body accumulate to a certain level and exceed the elimination limit of the body; the resulting oxidative stress causes damage in the fish.[5] Salinity is closely associated with the injury of immunity system, penetration regulation and tissue structure in fish leading to the heavy consumption of endogenous substance for survival.[6,7] Alkalinity affects fish physical and chemical balance, growth and development. When fish are exposed to water with excessive alkalinity, a large amount of mucus is secreted on the surface of the fish; bleeding hemorrhoids and even death occur.[8,9] Carbonate salts are the most abundant kind of salt in freshwater; these include bicarbonates and carbonates. Since carbonate salts have low solubility in water, water is mainly bicarbonate.[10] Alkalinity in the water usually refers to an amount of weak acid ions such as

[a]*Heilongjiang River Fisheries Research Institute of Chinese Academy of Fishery Sciences, Laboratory of Quality & Safety Risk Assessment for Aquatic Products, Ministry of Agriculture and Rural Areas, Harbin 150070, P. R. China. E-mail: liuhongbai@sina.com; wangym@cafs.ac.cn; Fax: +86-451-84604803; Tel: +86-451-84604803*

[b]*Department of Food Science and Engineering, College of Food Science and Technology, Shanghai Ocean University, Shanghai 201306, P. R. China*

† Electronic supplementary information (ESI) available. See DOI: 10.1039/c9ra08090b

‡ These authors contributed equally.

bicarbonate contained in water. At present, there are many distributions of saline–alkaline waters in the world. Although the aquaculture technology of saline–alkaline waters has achieved great development, a large amount of saline–alkali water resources cannot realize economic fish farming and be fully used.[11,12] As an economically important fish that lives in freshwater and one of the main edible fish species in China, crucian belongs to the *Carassius* genus in Perciformes: Sciaenidae. It is characterized by fast growth rate, good resistance to stress, strong tolerance to salt and alkali, and certain saline–alkali aquaculture potential.[13,14] These excellent properties make it an ideal material for the study of the adaptive evolution of salinity–alkalinity and the physiological mechanism of salinity–alkalinity-tolerant molecules.

With the rapid progress of "Omics" sciences in the past decades, transcriptomic, proteomic and genomics have become praiseworthy means to explore a whole reaction of a living creature in diverse ecologic change,[15–22] permitting the search for the intricate response of hundreds of transcripts, proteins and metabolites.[23–32] But genomics, transcriptomics and proteomics cannot meet the demand of interpretation of the intricate response in organisms after physiological and pathophysiological disturbance;[33–44] metabolomics has been highlighted as a powerful means to explore complicated theory systems and in medical modernization.[45–57] This method could monitor and quantify the changes of small-molecule metabolites, including fatty acids, amino acids, peptides, nucleic acids, organic acids, vitamins, and carbohydrates in organisms or biological samples in ultimate response to endogenous and exogenous factors.[58–67] Multiple resultant methods of metabolomics study have been used, such as chromatography, MS, magnetic resonance, fluorescence scattering, radioactivity detection and light scattering.[68–77] Liquid chromatography-mass spectrometry (LC-MS) is one of the metabolomic techniques widely used.[78–91] Metabolomic research studies have been largely fulfilled in human research for drug safety, toxicity evaluation, and disease diagnosis.[92–100] In recent years, various fish physiology and biochemical conditions, along with the consequences of pollutants and disease, have been smoothly detected by metabolomics strategy. However, such investigation has never been used to evaluate the molecular responses and mechanisms of fish exposed to CA in spite of offering a more well-rounded comprehension of what causes chronic harm to other living forms.

The aim of this research is to search for metabolomic biomarker and pathway changes in crucian under carbonate alkalinity exposure with three different concentration gradients using high-throughput serum metabolomics strategy, and then attempt to bring out molecular physiological mechanisms of saline–alkali tolerance in fishes, thus offering a scientific basis for physiologic and ecological research in crucian and implementing a rational management of water quality and bait utilization in the breeding process.

2. Methods

2.1 Chemicals and reagents

MS-grade acetonitrile and methanol were obtained from Thermo Fisher Scientific (Waltham, MA, USA). MS-grade formic acid was purchased from Sigma (St. Louis, Mo, USA). Ultrapure distilled water prepared from a Milli-Q purification system was used to prepare the mobile phase. MS-222, which is a special anesthetic for fish, was purchased from Biocrates Life Sciences (Innsbruck, AT). The assay kits of ammonia and urea were purchased from Sinopharm Chemical Reagent Co., Ltd. (Shanghai, China). The assay kits of alanine transaminase (ALT), glutamic–pyruvic transaminase (AST) were obtained from Tianjin Jinyao Amino Acid Co., Ltd. (Tianjin, China). The creatinine (CREA), urea nitrogen (UREA), blood glucose (GLU), total protein (TP), albumin (ALB) and glutamine (Gln) immunoassay (ELISA) kits were obtained from Senbeijia Bioengineering Institute (Nanjing, China). The assay kits of fish glutamine synthase (GS) carbamoyl phosphate synthase (CPS) were obtained from R&D systems (Minneapolis, MN, USA). The ELISA kits of superoxide dismutase (SOD), catalase (CAT), lactic dehydrogenase (LDH) and Na^+/K^+-ATPase were obtained from Cayman Chemical.

2.2 Live subject statement

This study was performed in strict accordance with the guidelines for the care and use of laboratory animals (No. 9972, Heilongjiang River Fisheries Research Institute of Chinese Academy of Fishery Sciences) and was approved by the Institutional Animal Care and Use Committee of Heilongjiang River Fisheries Research Institute of Chinese Academy of Fishery Sciences (Harbin, China).

2.3 Fish rearing

The study was conducted using two-year-old tail crucian (CC) (twenty-four female and twenty-four male) purchased by Jilin University (Jinglin, China), with average length of 15.5 ± 1.6 cm and an average weight of 50.2 ± 6.2 g. In the 7 day acclimation period before the experiment, adult fish were raised under the best growing conditions in gas-filled freshwater tanks filled with a mixture of dechlorinated tap water and reverse-osmosis filtered water (1/3 and 2/3, respectively), with an average temperature of $20\ ^\circ C \pm 1$ and a 12 h/12 h light/dark cycle. The fish were fed two times a day with commercial dry pellets (TetraMin, Melle, Germany).

2.4 Alkalinity exposure and sample collection

Forty-eight tail CC were divided into four equal groups as follows: three carbonate alkalinity groups and one control group, with six females and six males in every group. Fish were exposed to either CA or clean water for sixty days. Three exposure conditions were constituted in three distinct tanks containing CA of 20 mmol L^{-1} (CA20), 40 mmol L^{-1} (CA40), and 60 mmol L^{-1} (CA60). Each group of fish exhibited a healthy state during the exposure. Water effluent samples were collected every seven days of the exposure process, and normal feed was carried out. In addition, biochemical parameters in response to carbonate alkalinity in fish were detected for chronic impairment evaluation. On the 60^{th} day, the three CA groups and the control group of fish were administered MS-222 anesthesia, and 2 mL of whole blood was collected from the tail veins, then

placed in a 4 °C dark refrigerator and allowed to naturally separate. It is worth noting that the scalpel should not reach too deep to prevent the body from being stabbed when dissecting the belly of the crucian. Before removing the left body wall muscles, the liver and gill were taken in turn. After the branchial arch and hairs elimination, fish gill was immediately cut into slices approximately 0.3 cm^3 in size, and then was fixed with Bouin's solution, and stored at 4 °C for the next step.

2.5 Physical parameter detection

On day 0 and the 60th day of the experiment, the weights of each group of crucian were measured, and the weight gain rate of the fish body mass was calculated according to the following formula: weight gain rate = (Mt − Mo)/Mo × 100%; Mt indicates the quality of the fish at the end of the test, and Mo at the beginning of the test. On the 60th day of the experiment, the oxygen consumption rate and ammonia excretion rate of crucian in every group were determined by the closed-flow breathing method according to the following formula: $O_{CR} = (Do_o - Do_1) \times V/W$. O_{CR} is the rate of oxygen consumption (mg g^{-1} h^{-1}), Do_o is dissolved oxygen in the inlet (mg L^{-1}), Do_1 is dissolved oxygen in the outlet (mg L^{-1}), V is the water flow per unit time (L h^{-1}), and W is the mass of the experimental fish (g). $A_{ER} = (N_1 - N_0) \times V/W$. A_{ER} is the rate of ammonia excretion (μg g^{-1} h^{-1}); N_1 is dissolved ammonia nitrogen in the inlet (μg L^{-1}); N_0 is dissolved ammonia nitrogen in the outlet (μg L^{-1}); V is the water flow per unit time (L h^{-1}); and W is the mass of the experimental fish (g).

2.6 Biochemical parameter detection

The obtained blood was transferred into tubes straightway and centrifuged at 3000 rpm for 10 min at 4 °C within 3 h of collection for blood ammonia, urea, ALT, AST, CREA, UREA, GLU, TP and ALB detection according to kit instructions. The liver and branchia were weighed to 0.5 and 1 g, respectively. Normal saline was added in proportion of mass (g) : volume (mL) = 1 : 9, and the samples were homogenized at low temperature. The blood sample was centrifuged at 3000 rpm for 15 min under 4 °C, then the supernatants were used to detect tissue ammonia, urea, Gln, GS, CPS, SOD, CAT, LDH and Na^+/K^+-ATPase activity according to kit instructions. Biochemical indexes were performed using a Beckman (ProCX4) automatic biochemical analyzer and Synergy H1 microplate reader (Bio-Tek, USA).

2.7 Metabolomics study

Before UPLC-ESI-QTOF-MS, the whole blood drawn from the tail vein of crucian was stored in a refrigerator at 4 °C for 12 h, and then the serum supernatant (1.0 mL) was taken in a 5 mL centrifuge tube, and 4 mL of methanol (chromatographically pure) was added. The mixture was vortexed for 60 s, and then centrifuged at 10 000 rpm for 10 min. The gained supernatant was filtered by the 0.22 μm membrane and then analyed by the instrument for testing within 12 hours.

The serum samples were separated using a Waters Acquity UPLC BEH C18 column (2.1 mm × 100 mm, 1.7 μm) equipped with an AQUITY UPLC BEH C18 VanGuard Pre-Column pre-column (2.1 mm × 5 mm, 1.7 μm). The mobile phase A is water with 0.1% formic acid, and the mobile phase B is acetonitrile with 0.1% formic acid. The optimized gradient elution procedure was performed as follows: 0 to 2 min, 5% to 20% B; 2 to 3 min, 20% to 60% B; 3 to 11 min, 60% to 80% B; 11 to 12 min, 80% to 100% B; 12 to 13 min, 100% to 100% B; 13 to 13.1 min, 100% to 5% B; 13.1 to 15 min, 5% to 5% B. The column temperature was set to 30 °C, the injection was set to 5 μL, the flow rate was set to 0.3 mL min^{-1}, and the autosampler temperature was set to 4 °C. MS was performed on a Waters Micromass QTOF micro Synapt High Definition Mass Spectrometer (Manchester, UK) equipped with an electrospray ion source (EIS). The ionization mode is divided into electrospray positive and negative ion mode. The main parameters of positive and negative ion mode were set as follows: source voltages in positive and negative are respectively fixed at 5500 V and 4500 V; ion source temperature is 550 °C; de-clustered voltage (DP) is respectively set at 80 V and 60 V; collision energy (CE) is respectively set at 35 eV and 30 eV; collision energy expansion (CES) is set 15 eV. The spray gas is nitrogen, the auxiliary gas 1 is 55 psi, the auxiliary gas 2 is 55 psi, and the curtain gas is 35 psi. The primary mass spectrometer has a scan range of 80–1200 Da. The IDA sets the 8 peaks with a response value exceeding 100 cps for the second-order mass spectrometry. The sub-ion scan range is 50–1200 Da, and dynamic background subtraction (DBS) is turned on. The data were collected at 1 MS spectrum every second with a scan time of 0.2 s, an inter-scan delay of 0.1 s, and a lock spray frequency of 10 s. The data acquisition software used was Analyst TF 1.6 software.

2.8 Data processing

The original MS spectral data were firstly converted to a common data format in Mass Hunter and subjected to the process of noise filtering, peak detection, removal of isotope masses and alignment of retention time (Rt) and mass (m/z) using MetaboAnalyst (V 4.0, Montreal, Quebec, Canada) with Peakview 2.0/Masterview 1.0 software and Progenisis QI 2.0. Each ion intensity was normalized relative to the total ion count and formed a data matrix containing Rt, m/z value, and the normalized peak area. The data matrix was imported and handled by SIMCA-P V13.0 (Umetrics AB, Malmo, Sweden). Pattern recognition analysis, including unsupervised principal component analysis (PCA) and supervised orthogonal partial least squares discriminant analysis (OPLS-DA), was used for discovery of differently expressed metabolites. A score plot (S-plot) was applied to envisage the results that could mirror differences among control groups and different CA exposure groups and thus demonstrate the variables that are promoted to the classification, which appraises the model quality by the $R2$ and $Q2$ values calculation. A variance importance for projection (VIP)-plot was generated following OPLS analysis-plot, and the p-values greater than 1 were used to choose the potential metabolites. Metabolite structural identification was assigned based on the accurate mass and mass spectrometric fragmentation patterns. Utilizing HMDB, KEGG, Chemspider,

LIPIDMAPS as well as Scripps Center for mass spectrometry, the selected metabolites were qualified. The information of biochemical reactions associated with the response of crucian to CA exposure was obtained using the Kyoto Encyclopedia of Genes and Genomes (KEGG). The differential metabolites concentration alteration, interaction and pathway analysis was

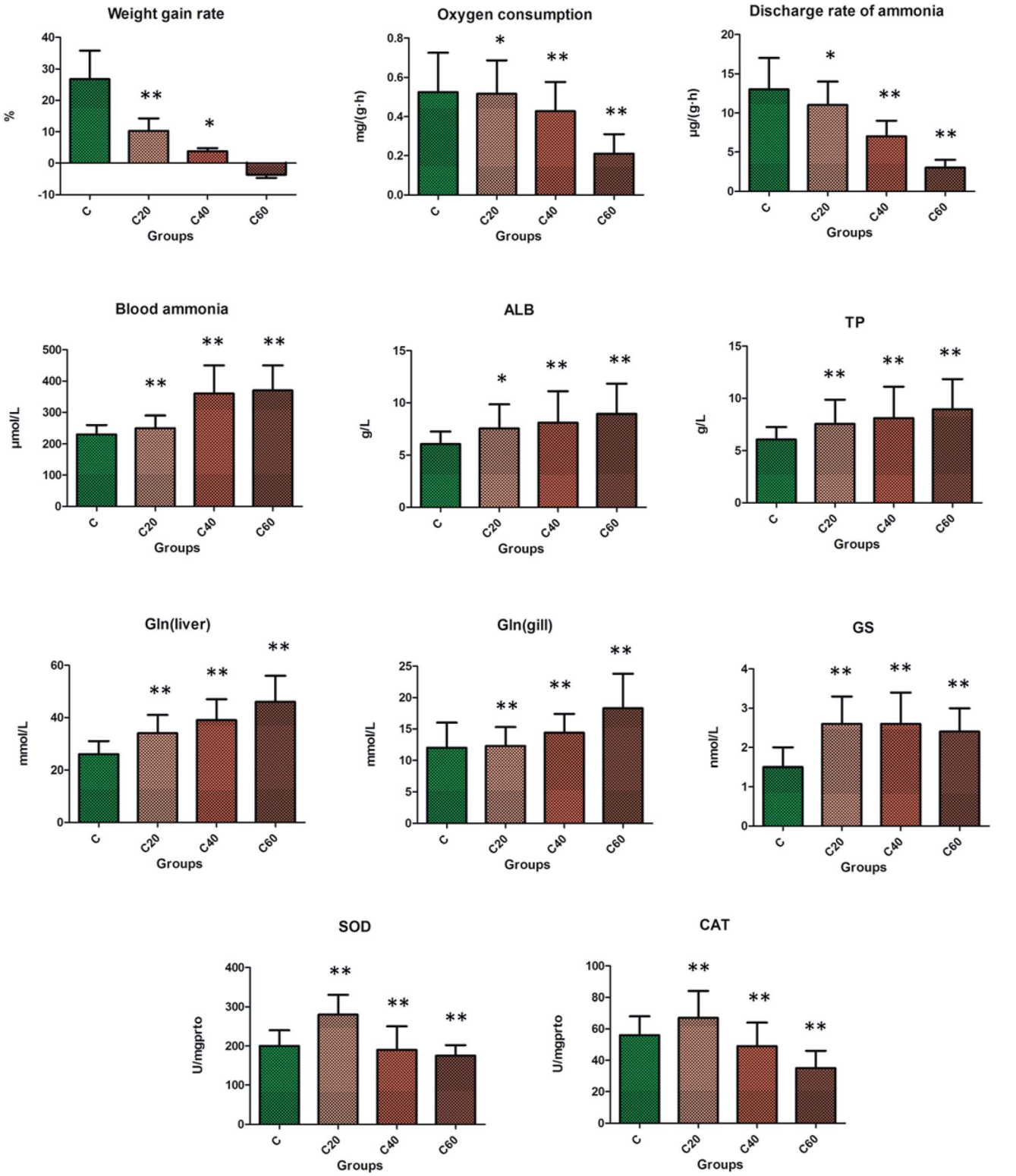

Fig. 1 A comparison of weight gain rate, oxygen consumption, the discharge rate of ammonia content, blood ammonia, TP, ALB, Gln of the liver and gills, GS, SOD, and CAT between a control and different CA exposure groups. * stands for significant difference ($p < 0.05$) compared to the control group, ** stands for very significant difference ($p < 0.01$) compared to the control group.

disposed by MetaboAnalyst 4.0. All statistical analyses were computed by the two-tailed, two-sample Student's *t*-test. The resulting data are presented as mean ± standard deviation (SD). Data with *p*-values less than 0.05 were considered to be statistically significant, and *p*-values less than 0.01 were believed to indicate highly significant difference.

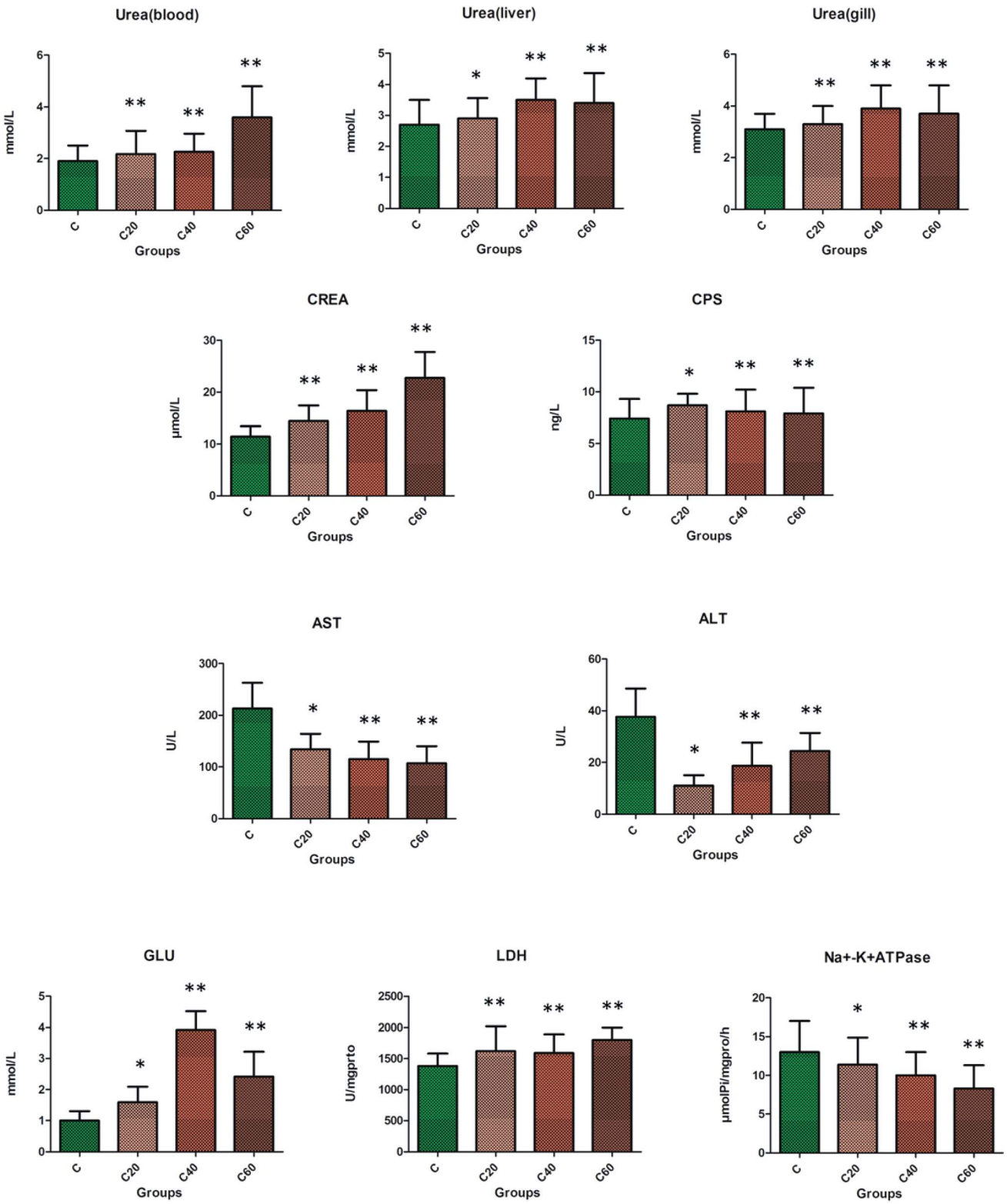

Fig. 2 A comparison of urea in the liver, gills and blood, CREA, CPS, ALT, AST, GLU, LDH and Na^+/K^+-ATPase between a control and different CA exposure groups. * stands for significant difference ($p < 0.05$) compared to the control group, ** stands for very significant difference ($p < 0.01$) compared to the control group.

3. Results

3.1 Effect of alkalinity exposure on physical indicators

In comparison with the control group, the level of weight gain rate, oxygen consumption, and discharge rate of ammonia were significantly decreased as the concentration increased, but the weight gain rate was obviously reduced in the CA20 group ($p < 0.01$). The oxygen consumption and discharge rate of ammonia in the CA40 group were significantly decreased in the fish under CA exposure compared with the control group ($p < 0.01$).

3.2 Effect of alkalinity exposure on biochemical indicators

As shown in Fig. 1, the blood ammonia, TP, and Gln of liver and gills were evidently heightened in the CA20 group compared with the control group ($p < 0.01$), which might have been induced by damage in crucian. At CA20 level, the ALB, GS, SOD and CAT were markedly increased compared with the control group ($p < 0.01$), and then with the increase of concentration, the content of the above four indicators gradually decreased, with the level of SOD and CAT reduced compared to that of the control group and the level of ALB and GS remaining elevated compared to that of the control group. As shown in Fig. 2, the urea in blood, liver and gill;

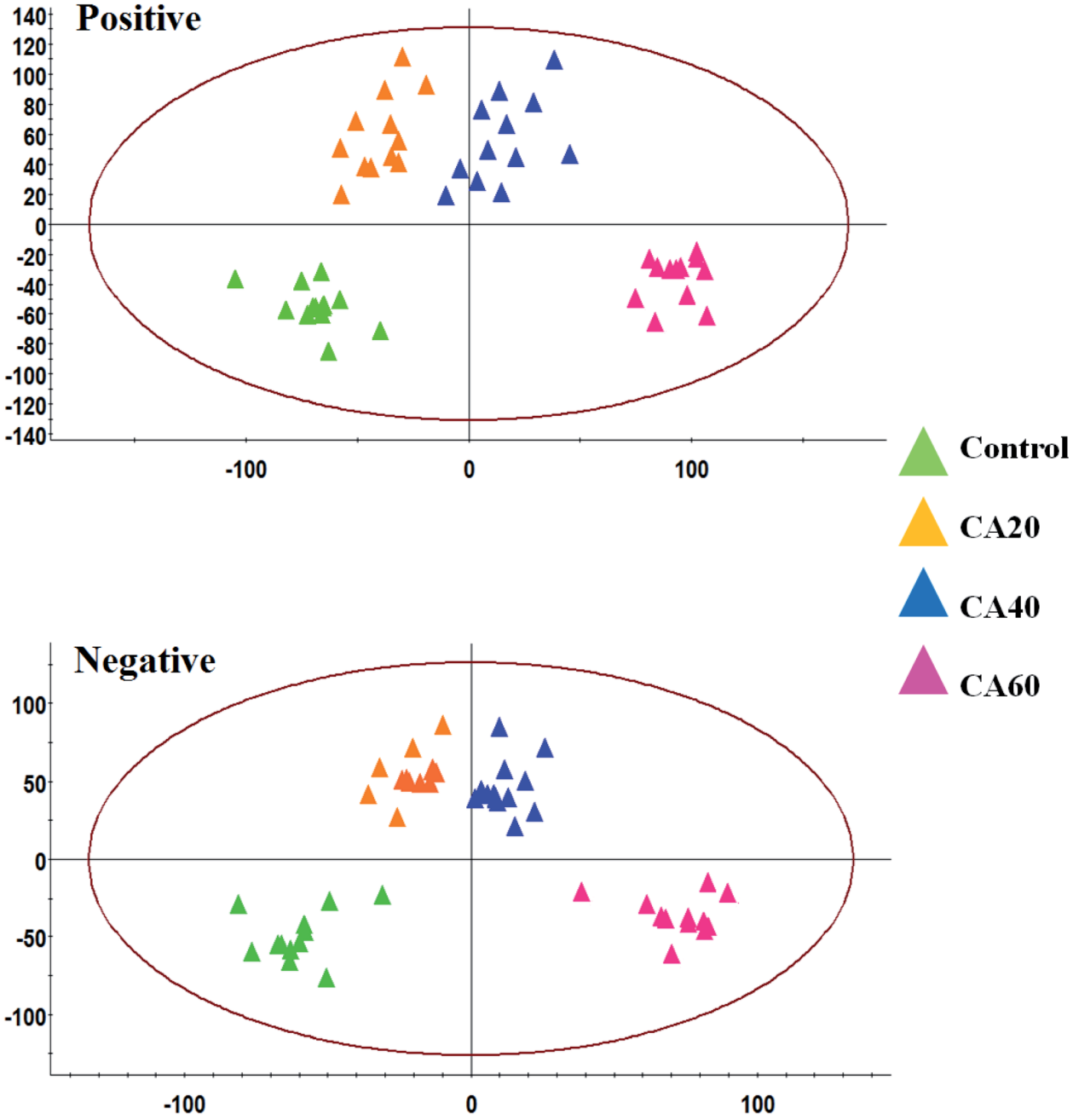

Fig. 3 PCA score plots of serum sample UPLC-MS spectra data between a control and different CA exposure groups under positive and negative mode.

CREA; CPS; Glu and LDH in the CA group were increased compared with control group, with CPS from the CA40 to CA60 ($p < 0.01$) and Glu in CA60 ($p < 0.01$) groups markedly decreased, but they were still higher than that of the control group. The ALT, AST and Na^+/K^+-ATPase in CA group were decreased compared with the control group, with ALT from CA40 to CA60 ($p < 0.01$) markedly increased but still lower than that of the control group.

3.3 Effect of alkalinity exposure on serum metabolomics

Serum analysis was obtained well resolved with good peak shape, intensity and separation in total ion chromatograms (TICs) under the optimized chromatographic and MS conditions. Unsupervised PCA in both modes was performed on all of the samples in the research. The results show that 46.7% and 47.2% of the total variance is explained by the first two

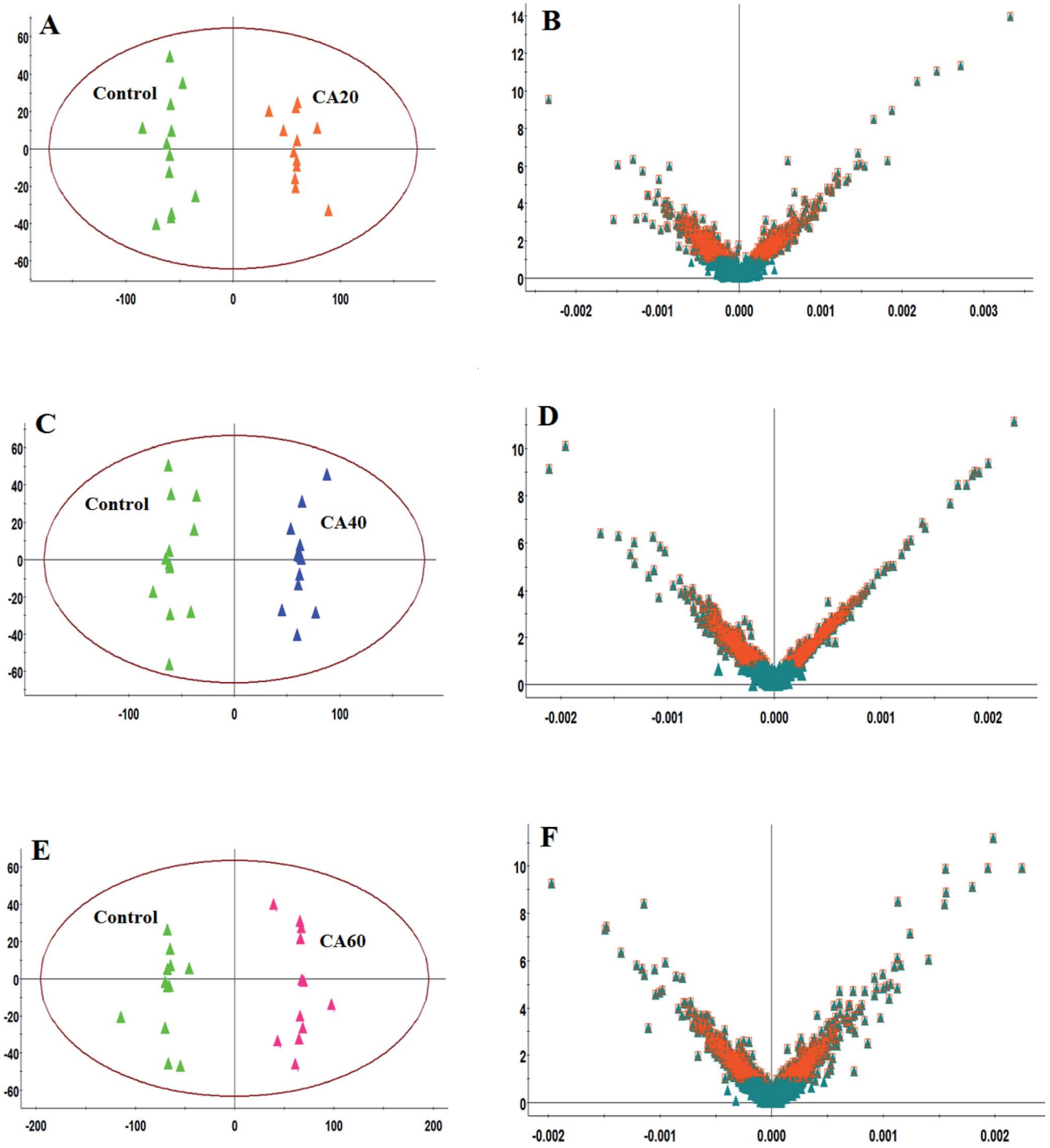

Fig. 4 OPLS-DA score plot and VIP-plot of OPLS-DA model between control and different CA exposure groups in positive mode. (A), (C) and (E): OPLS-DA score plot; (B), (D) and (F): VIP-plot of OPLS-DA model. The size and format meet the requirements.

principal components, respectively. The analytical method was strong and possess favorable repeatability and stability from QC samples in the preliminary experiment, which were found to be bunched familiarly in both modes of the PCA score plots. As shown in Fig. 3A and B, the different CA concentration group and the control group in the score plots present intelligible parting, which indicate that crucian under CA exposures present an evident difference in the serum metabolic profiles. As the concentration increased, blood samples from different groups gradually moved away from the control group, reaching the maximum when CA was 60 mmol L^{-1}.

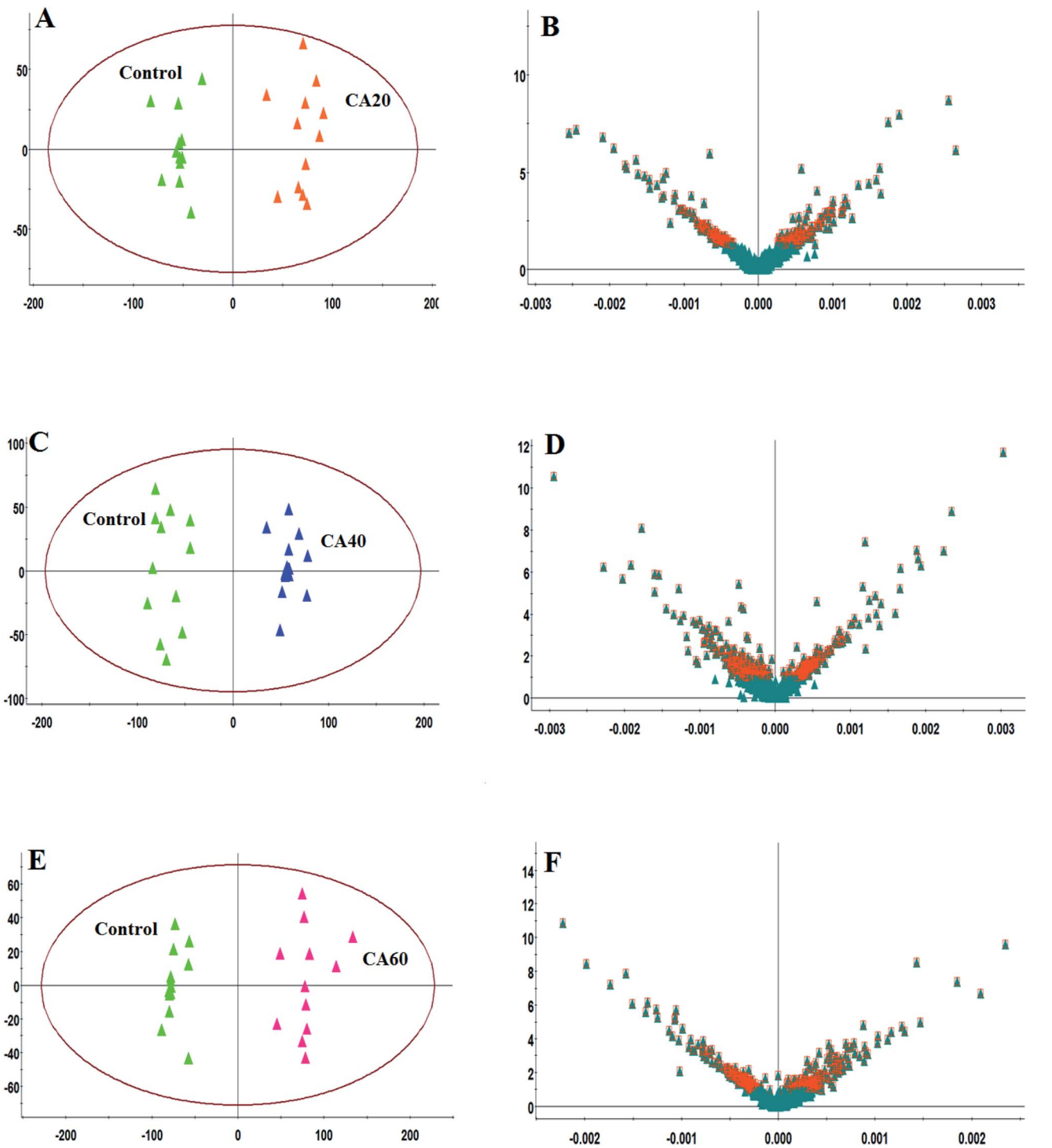

Fig. 5 OPLS-DA score plot and VIP-plot of OPLS-DA model between control and different CA exposure groups in negative mode. (A), (C) and (E): OPLS-DA score plot; (B), (D) and (F): VIP-plot of OPLS-DA model. The size and format meet the requirements.

3.4 Potential metabolite search and identification

To further highlight the discrepancy and select the metabolites, OPLS-DA models were instituted and applied between the model and other groups to improve the variation. In Fig. 4 and 5 the OPLS-DA score plots show a clear excision between the control and other CA exposures groups from 20 mmol L^{-1} to 60 mmol L^{-1} without any overlap in either the positive or negative modes, which designated that there was a disturbation of the serum metabolic profile in CA exposures groups. The OPLS-DA outcome was in line with the above PCA score plots. The *R2X* and *R2Y* values were close to 1, and *Q2* values were more than 0.5 in the OPLS-DA models, respectively, which indicated that the models were steady and possess predictive abilities. Then, VIP plot followed by OPLS analysis plot and the *p*-values were obtained to seek and identify metabolites as biomarkers that had a vital effect on the group separation, which are shown in Fig. 4B, D, F and 5B, D, F. With VIP values > 1.0 and *p*-values < 0.05, 27 metabolites in the serum were deemed as potential metabolites associated with CA exposure effects. Metabolite information, such as ion mode, Rt (min), error, compound name and formula are shown in Table S1.† As the concentration increases, fourteen metabolites, including citric acid, glucose, pyruvic acid, uridine, L-leucine, Cer (d18:0/18:0), homocysteine, isocitric acid, arginine, LysoPC (15:0), LysoPC (18:0), LysoPE (0:0/20:0), LysoPC (18:1(9Z)), and sphingosine showed a marked decrease, and nine metabolites, including uric acid, lactic acid, asparagine, glutamine, phenylalanine, tyrosine, arachidonic acid, lysine and taurocholic acid showed a marked increase. In addition, the level of palmitic amide, valine, corticosterone and glycerophosphocholine were firstly increased and then decreased from 20 mmol L^{-1} to 60 mmol L^{-1} CA. The alteration of these metabolites stimulated by CA exposures was carried out to demonstrate the comparative level relationships and discrepancy in the heatmap of Fig. 6.

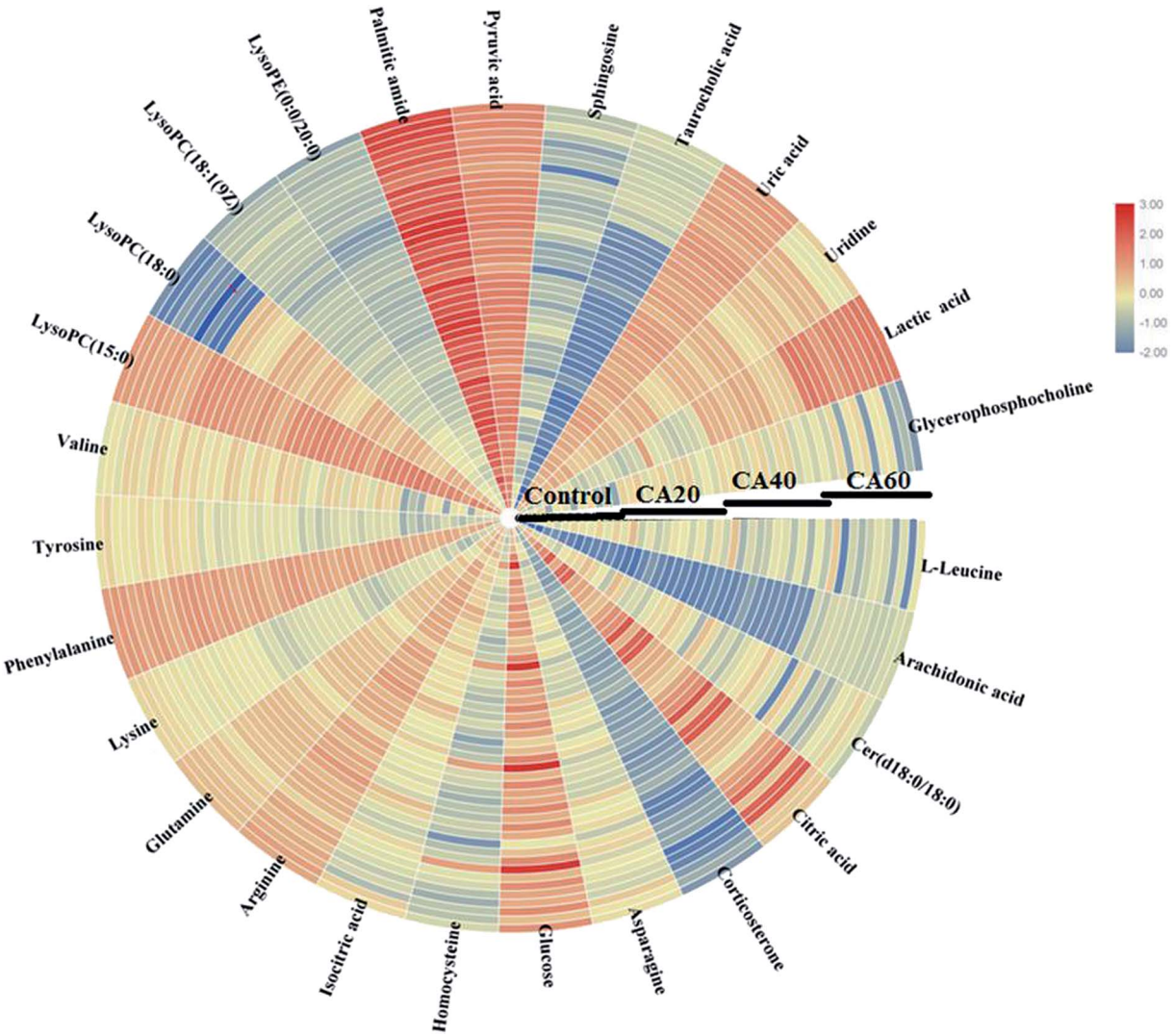

Fig. 6 The heatmap visualization of twenty-seven metabolites in serum samples from a control and model group. Different colors indicate changes in the relative metabolite content values. Red indicates an increase in the content, and blue indicates a decrease in the content.

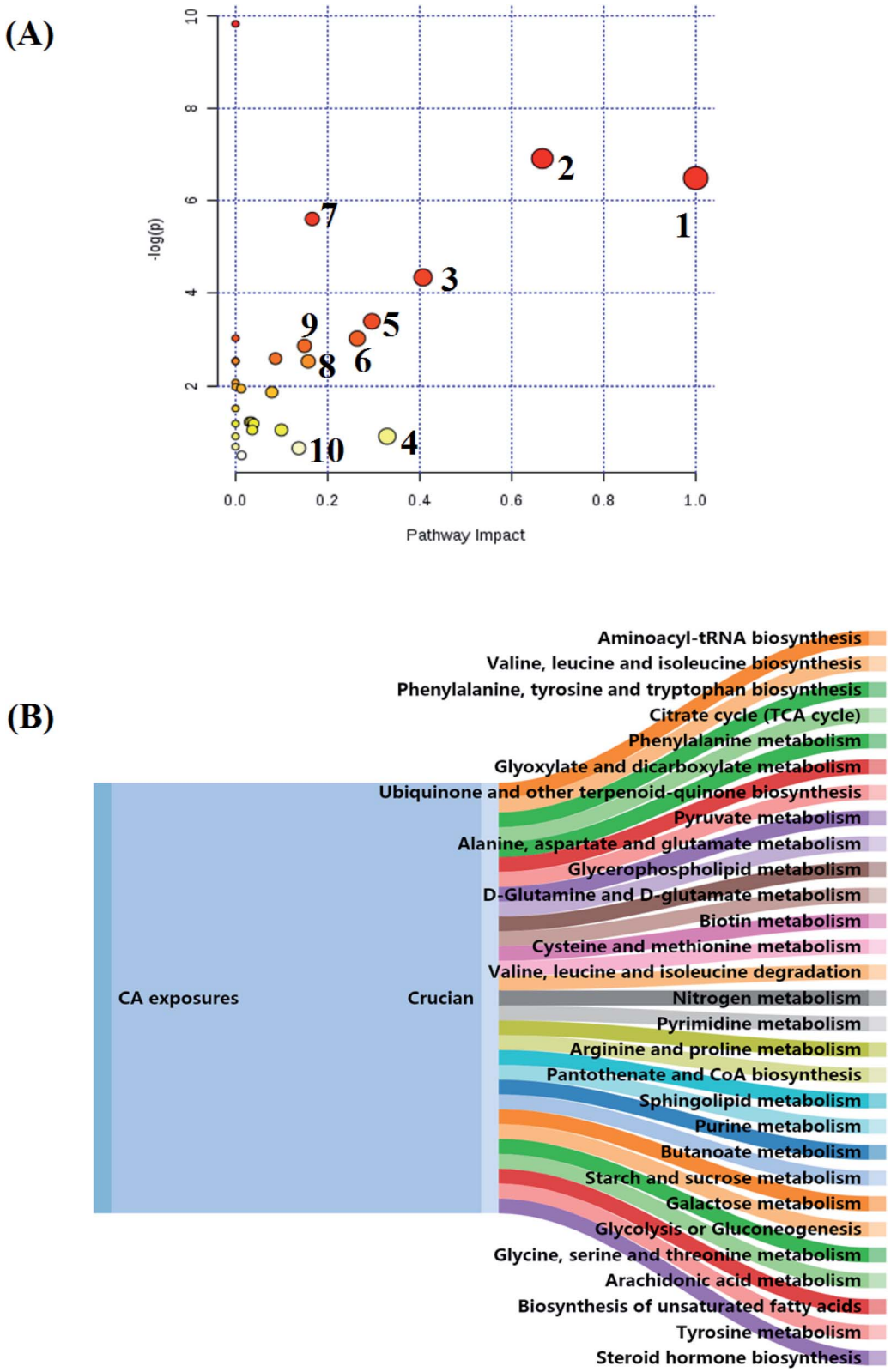

Fig. 7 (A) Significant pathway analysis of metabolic variations in crucian under CA exposure: (1) phenylalanine, tyrosine and tryptophan biosynthesis; (2) valine, leucine and isoleucine biosynthesis; (3) phenylalanine metabolism; (4) arachidonic acid metabolism; (5) glyoxylate and dicarboxylate metabolism; (6) pyruvate metabolism; (7) citrate cycle (TCA cycle); (8) cysteine and methionine metabolism; (9) alanine, aspartate and glutamate metabolism; and (10) tyrosine metabolism. (B) Exploring all the metabolomic pathway in crucian under carbonate alkalinity exposures depicted by Sankey diagram.

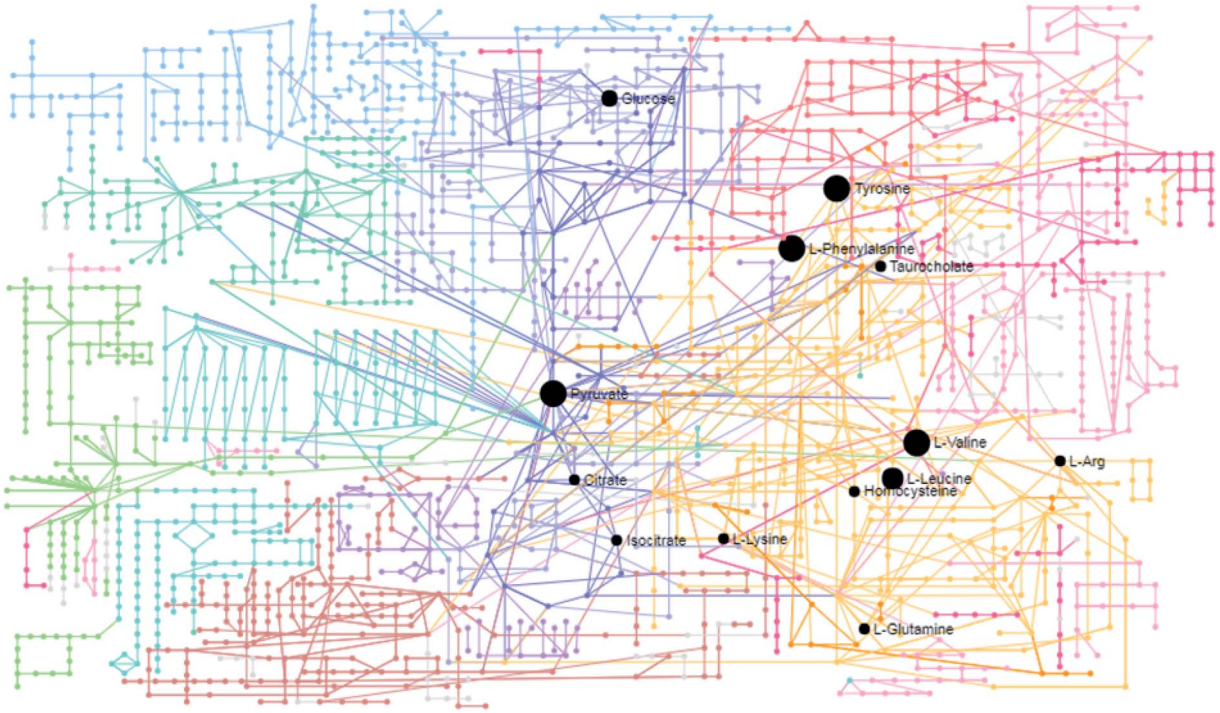

Fig. 8 The KEGG global metabolic network related to crucian under CA exposure.

3.5 Pathway interpretation

All the distinct metabolites were resolved by MetaboAnalyst software to bring to light their association with metabolic pathways. Relative pathways with an impact-value greater than 0.1 that explore the metabolic effects of CA exposure are shown in Fig. 7A; it comes down to phenylalanine, tyrosine and tryptophan biosynthesis; valine, leucine and isoleucine biosynthesis; phenylalanine metabolism; arachidonic acid metabolism; glyoxylate and dicarboxylate metabolism; pyruvate metabolism; citrate cycle (TCA cycle); cysteine and methionine metabolism, alanine, aspartate and glutamate metabolism; and tyrosine metabolism. In Fig. 7B, all the disorder pathways are shown to highlight the pathway changes in crucian during CA exposure. Then, integrated network analysis of CA exposure in crucian was performed to outline the biochemical relationships. From the KEGG global metabolic network, which can map metabolites in crucian under CA exposure and enzymes/KOs (KEGG Orthologs; Fig. 8), it is appropriate to confirm results from common metabolomics and metagenomics studies mostly relating to amino acid metabolism, lipid metabolism and glucose metabolism. The relationships of genes and main metabolites of serum samples in crucian under CA exposure are demonstrated in Fig. 9A, mainly referring to arachidonic acid, L-arginine, citric acid, L-lysine, L-glutamine and corticosterone with gene betweenness of 214 699.2, 136 361.8, 146 454.6, 54 034.97, 111 102.8 and 92 312.9, respectively. The metabolite–metabolite interaction network based on reactions from similar chemical structures and similar molecular activities that highlight potential functional relationships between a wide set of annotated metabolites is shown in Fig. 9B; five metabolites, including pyruvic acid, citric acid, L-lysine, L-glutamine and L-arginine, stand out with 233, 132, 114, 105 and 102 degrees.

4. Discussion

pH is generally considered to be one of the most important environmental factors in fish farming; with pH changes directly affecting fish respiration, excretion and other physiological indicators. When fishes live in the suitable pH range environment, the main enzyme activity in corresponding tissues and organs activity were increased for maintaining the metabolism.[123] The pH value caused by some chemicals beyond the scope can lead to the water content changes, it may even be turned into some toxic substances, affecting the water quality and condition of the dissolved oxygen in the water.[124] If the ion concentration in the water is higher that exceeds the plasma osmotic pressure in the fish, a large amount of salt enters the fish causing water loss in the body and the osmotic pressure increase. Due to osmotic adjustments of the body, a large amount of salt absorbed in the body cannot be discharged and the lost water cannot be replenished, which leads to destruction of the body's osmotic pressure balance and blood concentration, thus leading to damage to the body and even death. The same situation can be seen from the rate of weight gain, which prevents fish from breathing, resulting from the decline in oxygen consumption rate. The results showed that the oxygen consumption rate of crucian remained basically unchanged when CA was 20 mmol L^{-1}, indicating that saline–alkaline tolerant fish could adapt to the high-saline–alkali environment by maintaining their physiological stability within the appropriate saline–alkaline range. With the increase of saline–

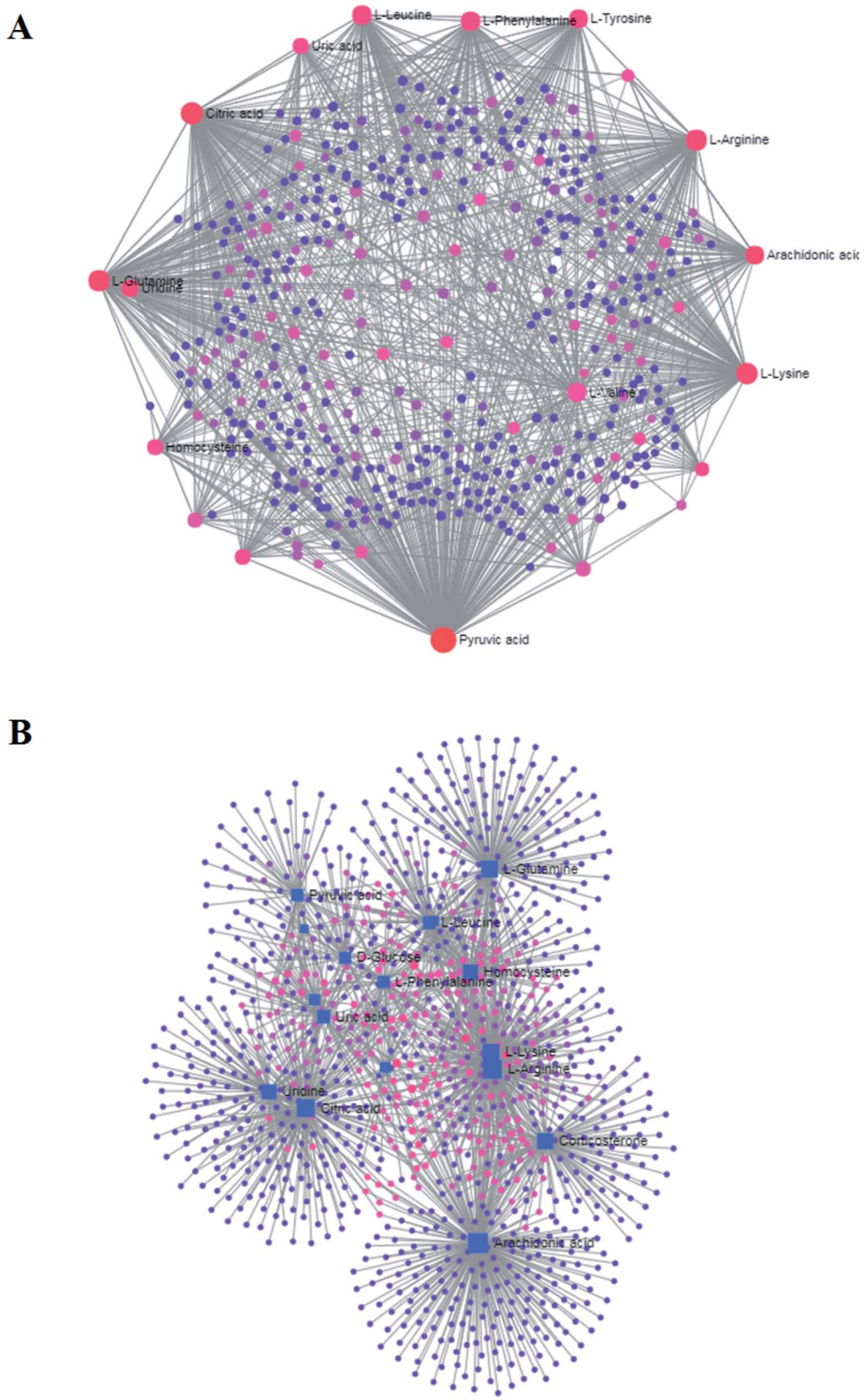

Fig. 9 (A) Metabolite–gene and (B) metabolite–metabolite interaction networks associated with crucian changes after CA exposure.

alkaline, oxygen consumption was decreased, which indicated that the metabolism of crucian was abnormal.[125] From the results of metabolomics analysis, it can be found that the content of lactic acid increases with the increase of CA concentration, indicating that salt-alkali stress can inhibit aerobic respiration and increase the level of anaerobic

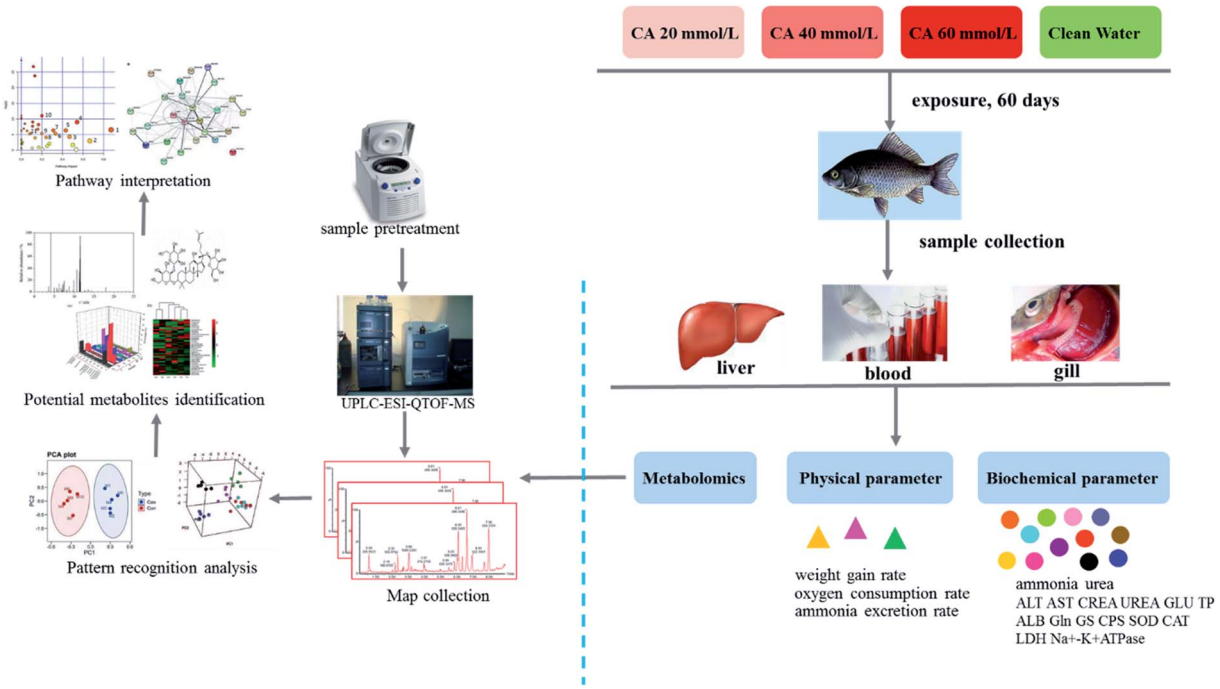

Fig. 10 The process of exploring the metabolic biomarkers and pathway changes in crucian under carbonate alkalinity exposure using metabolomics analysis.

respiration.[126] When CA is 60 mmol L^{-1}, weight is also significantly reduced. Recent studies have shown that the accumulation of ammonia under the carbonate environment caused by ion concentration changes *in vivo* and *in vitro* gives rise to toxic effects in fishes. The toxicity is manifested as the ability of NH^{4+} to replace K^{+} in the ion transporter and damage the electrochemical gradient in the central nervous system. At the same time, it was suggested that the ammonia poisoning death of fish may be related to oxidative damage and immunosuppression.[127,128] In this study, the concentration of ammonia in the blood of crucian increased with the increase of alkalinity at 40 mmol L^{-1}, and the increase was more severe. It can be seen from the survival of the experimental fish that crucian has good adaptability to the saline–alkaline environment below 60 mmol L^{-1}. The ammonia excretion rate decreased gradually with the increase of alkalinity. When CA was 60 mmol L^{-1}, the ammonia excretion rate was the lowest, while the blood ammonia content was relatively the highest. The effect of pH on ammonia excretion rate is mainly realized by the metabolic rate of fish tissues. Ammonia in the fish is catalyzed by CPS to produce a series of biochemical reactions such as transoxylated phosphoric acid, and finally produces urea, which reaches the kidney through blood circulation and then leaves the body. In addition, gills are also a vital organ for excreting urea *via* special proteins for urea transport.[129]

Mass spectrometry-based metabolomics has been used to discover metabolic biomarkers that reveal disease mechanisms,[130–135] as well as for diagnosis,[136–142] prognosis,[143–146] and treatment.[147–149] In this study, urea levels in the blood, liver and gill of crucian were increased significantly with CA20 mmol to 60 mmol exposure, accompanied by the increase of blood ammonia concentration after the beginning of stress, which verified that the urea metabolism pathway of ammonia in crucian began to occur on the biochemical level. The process of the study shown in Fig. 10 illustrates the exploration of the metabolic biomarkers and pathway changes in crucian under carbonate alkalinity exposure using metabolomics analysis. From CA20, the activity of CPS enzyme in liver was significantly improved, which also proved that the urea metabolism pathway of crucian for ammonia discharge could be rapidly started in CA20. Within the range of CA40 to CA60, although CPS activity was significantly increased compared with that of the control group, it was also decreased compared with that of CA20 in control group, indicating that with the increase of alkalinity change, the metabolism of crucian gradually showed chronic injury in the environment of high CA concentration under a long time.[150] In addition to urea metabolism pathway, with the increase of blood ammonia, the concentration of glutamine in liver and gill also began to rise from CA20, and the activity of liver GS enzyme began to rise rapidly, indicating that the ammonia reduction mechanism converting ammonia into glutamine has been started and played different effects on ammonia reduction in response to saline and alkaline stress.[151] Glutamine on the cell membrane has good permeability. Animal ammonia that is mainly in the form of glutamine is transported to the discharge area, and glutamine in fish will be transported to the gills. It is converted to ammonia after enzyme action, then discharged from the gill epithelium with the help of the blood–water diffusion gradient or a transport protein carrier. Glutamine not only is the main source of amino acids in

extracellular fluid, but also improves immune cell function, stress reaction, and a variety of physiological functions.[152] Fish ammonia poisoning death is closely associated with oxidative damage and immunosuppression induced by swelling of stellate glial cells. The result that crucian began to synthesize glutamine after CA20 stress may not be just in order to reduce the toxic effect of ammonia on the body; the glutamine can also participate in regulating the crucian's ability to adapt to stress and ensuring body survival. The decreased GS level in liver and gill under CA60 indicates that the increase of alkalinity to a certain extent can slow down the metabolism of glutamine in fish. As the concentration of CA increases, the content of arachidonic acid also increases, and the inflammatory response in the body becomes more and more intense.[153]

As the key amino transferases in the body of fish, the activity of ALT and AST not only reflect the metabolic status of amino acids in fish, but also indirectly embody the health status of liver function in fish. In this study, the activity of ALT and AST in serum in the CA exposure groups was outstandingly lower than that of the control group, indicating that the metabolism of liver and pancreas of crucian was inhibited.[154] CREA level is used to diagnose renal function, with the increased level signifying the decrease of glomerular filtration function caused by various reasons. With the increase of CA, CREA level in the CA exposure groups was significantly increased, indicating that the kidney function of crucian is impaired. The changes of serum UREA content reflected the protein metabolism of the animal. In this study, the serum UREA in each CA group was higher than that in the control group, and the difference between the high-concentration CA exposure groups and the control group was significant, indicating that the CA 60 saline–alkali stress had a significant inhibitory effect on the protein metabolism of crucian.[155–156] Protein, as an important component in serum, plays a vital role in fish physiology and immune system. Serum TP and ALB are mainly involved in maintaining the stability of plasma colloid osmotic pressure in the body and the balance of PH in the blood vessels. In this experiment, the serum TP and ALB levels in the CA groups were significantly higher than those in the control group, indicating that the increase of carbonate alkalinity concentration in water changed the osmotic pressure of the body and stimulated the body to enhance the ALB level. Studies have shown that amino acids act as energy source in fish osmotic pressure regulation.[157] Metabolic substrates play a major role, and non-essential amino acids appear to be the preferred amino acids for energy metabolism. Amino acids that serve as substrates for energy metabolism include branched-chain amino acids in skeletal muscle, members of the glutamic acid family, such as Pro and Glu, and the main substrates of hepatic gluconeogenesis, such as Ala. It is noted that the response of fish to CA stimulation is a process of slowly regulating autonomic adaptation. The down-regulated levels of L-leucine, pyruvic acid and homocysteine and the up-regulated levels of phenylalanine, tyrosine, valine and glutamine in crucian suggested that amino acid metabolism during CA stimulation process presented an abnormal state in order to adapt to changes in the environment at an early stage, which then inhibits the level of fish metabolism, which manifests in terms of osmotic pressure regulation capacity, antioxidant capacity, ammonia metabolism and liver function.[158]

Changes in LDH levels directly affect energy metabolism in the body. Tissue lesions and damage can cause an increase in cell membrane permeability, resulting in the release of large amounts of LDH into the blood. In this experiment, serum LDH levels in groups exposed to different concentrations of CA were significantly higher than those in the control group, indicating that energy metabolism in the body was damaged by carbonate alkalinity exposure.[159] As an important part of the animal detoxification system, AKP is involved in the digestion, absorption and transport of nutrients in animals. The results showed that the AKP level in the CA exposure groups was significantly higher than that in the control group, which indicates that the toxic effect of CA stress on the crucian stimulates the AKP level to increase in order to alleviate the body damage at CA20. With the increase of carbonate alkalinity from 20 mmol L^{-1} to 40 mmol L^{-1}, the ATP level is significantly reduced indicating that CA exposure environment will cause chronic damage to the body.[160] Meanwhile, as the main metabolites of the three major nutrients, the contents of citric acid, isocitric acid and pyruvic acid in fish gradually decreased as the concentration of CA increased, indicating that the metabolic cycle of carbohydrates, proteins and lipids for energy production was hindered under salt-alkali stress and thus presents chronic damage in crucian. Compared with the control group, the activity of SOD and CAT in the CA20 group was significantly increased, and in the CA40 and CA60 groups was significantly decreased, which indicated that the low concentration of CA could promote the feedback resistance mechanism of crucian during the stress response, and the antioxidant enzyme activity was inhibited, caused by oxidative damage to the body as the salinity concentration increased.[161]

For many countries in the world that lack freshwater, improving the ecological environment in these saline–alkali areas, broadening the fishing areas and gradually using the barren waters is a vital way to maintain the sustainable development of fisheries. At present, the measures to improve the water conditions of saline–alkali ponds mainly include the following methods: using river water and groundwater resources to directly dilute various ion concentrations in saline–alkali waters; increasing the relative height of fish ponds and groundwater levels; using a film to cut off the interface between pond water and saline–alkali soil, reducing the return of salt due to excessively high groundwater levels; applying organic and inorganic fertilizers; and planting some green manure plants that can reduce alkali and discharge salt. Crucian is an omnivorous fish with high nutritional value. Its distribution is extremely wide due to its strong adaptability, and it is also found in strongly alkaline water. This kind of fish has high research value. It is important to implement basic research on increasingly important factors, such as fish density, temperature, and pH tolerance range. Furthermore, it is helpful to establish standardized fish breeding models and technical specifications for different saline–alkali water quality conditions, select fish species in the correct way, and avoid

emergencies such as fish disease and death due to saline–alkali problems.

5. Conclusions

In the present study, we demonstrate metabolomic biomarker and pathway changes in crucian under carbonate alkalinity exposure. A total of twenty-seven endogenous metabolites and several vital pathways, such as amino acid synthesis and metabolism, arachidonic acid metabolism, glyoxylate and dicarboxylate metabolism, pyruvate metabolism and citrate cycle (TCA cycle), were identified highlighting that CA can change the normal metabolism of fish, affecting the osmotic pressure regulation capacity, antioxidant capacity, ammonia metabolism and liver and kidney function to adapt to the CA exposure environment at low concentrations and causing chronic damage to the body with increased concentrations of CA. The metabolomic strategy offers precious information about the chronic response of fish to CA exposure. This potentially powerful and non-lethal tool helps us better understand the molecular interactions for future environmental hazard appraisals of pollutants and for environmental control.

Conflicts of interest

There are no conflicts to declare.

Acknowledgements

This study was supported financially by the Special Scientific Research Funds for Central Non-profit Institutes, Heilongjiang River Fishery Research Institute (HSY201402), the special fund for Construction of Chinese Modern Agricultural Industry Technology System (CARS-46) and the Special Scientific Research Funds for Central Non-profit Institutes, Chinese Academy of Fishery Sciences (2016HY-ZD1205).

References

1 J. Kaur, M. Khatri and S. Puri, Toxicological evaluation of metal oxide nanoparticles and mixed exposures at low doses using zebra fish and THP1 cell line, *Environ. Toxicol.*, 2019, **34**(4), 375–387.

2 E. G. Canli, A. Dogan and M. Canli, Serum biomarker levels alter following nanoparticle (Al_2O_3, CuO, TiO_2) exposures in freshwater fish (*Oreochromis niloticus*), *Environ. Toxicol. Pharmacol.*, 2018, **62**, 181–187.

3 U. K. Saleem Raja, V. Ebenezer, A. Kumar, *et al.*, Mass mortality of fish and water quality assessment in the tropical Adyar estuary, South India, *Environ. Monit. Assess.*, 2019, **191**(8), 512.

4 C. M. Wood, P. Wilson, H. L. Bergman, *et al.*, Obligatory urea production and the cost of living in the *Magadi tilapia* revealed by acclimation to reduced salinity and alkalinity, *Physiol. Biochem. Zool.*, 2002, **75**(2), 111–122.

5 T. A. Blewett, C. M. Wood and C. N. Glover, Salinity-dependent nickel accumulation and effects on respiration, ion regulation and oxidative stress in the galaxiid fish, *Galaxias maculatus*, *Environ. Pollut.*, 2016, **214**, 132–141.

6 Y. Y. Chen, A. C. Cheng, S. A. Cheng, *et al.*, Orange-spotted grouper *Epinephelus coioides* that have encountered low salinity stress have decreased cellular and humoral immune reactions and increased susceptibility to *Vibrio alginolyticus*, *Fish Shellfish Immunol.*, 2018, **80**, 392–396.

7 E. J. Reynolds, D. S. Smith, M. J. Chowdhury, *et al.*, Chronic effects of lead exposure on topsmelt fish (*Atherinops affinis*): Influence of salinity, organism age, and relative sensitivity to other marine species, *Environ. Toxicol. Chem.*, 2018, **37**(10), 2705–2713.

8 J. D. Ouellet, M. G. Dubé and S. Niyogi, Influence of elevated alkalinity and natural organic matter (NOM) on tissue-specific metal accumulation and reproductive performance in fathead minnows during chronic, multi-trophic exposures to a metal mine effluent, *Ecotoxicol. Environ. Saf.*, 2013, **95**, 104–112.

9 T. L. Linbo, D. H. Baldwin, J. K. McIntyre, *et al.*, Effects of water hardness, alkalinity, and dissolved organic carbon on the toxicity of copper to the lateral line of developing fish, *Environ. Toxicol. Chem.*, 2009, **28**(7), 1455–1461.

10 I. Ruiz-Jarabo, S. F. Gregório, P. Gaetano, *et al.*, High rates of intestinal bicarbonate secretion in seawater tilapia (*Oreochromis mossambicus*), *Comp. Biochem. Physiol., Part A: Mol. Integr. Physiol.*, 2017, **207**, 57–64.

11 P. J. G. Henriksson, B. Belton, K. M. Jahan, *et al.*, Measuring the potential for sustainable intensification of aquaculture in Bangladesh using life cycle assessment, *Proc. Natl. Acad. Sci. U. S. A.*, 2018, **115**(12), 2958–2963.

12 O. O. Alawode and I. B. Oluwatayo, Development Outcomes of Fadama III among Fish Farmers in Nigeria: Evidence from Lagos State, *Eval. Program Plann.*, 2019, **75**, 10–19.

13 H. Dong, G. Lu, Z. Yan, *et al.*, Molecular and phenotypic responses of male crucian carp (*Carassius auratus*) exposed to perfluorooctanoic acid, *Sci. Total Environ.*, 2019, **653**, 1395–1406.

14 Q. Le, J. Hu, X. Cao, *et al.*, Transcriptomic and cortisol analysis reveals differences in stress alleviation by different methods of anesthesia in Crucian carp (*Carassius auratus*), *Fish Shellfish Immunol.*, 2019, **84**, 1170–1179.

15 J. Tica, E. J. Bradbury and A. Didangelos, Combined Transcriptomics, Proteomics and Bioinformatics Identify Drug Targets in Spinal Cord Injury, *Int. J. Mol. Sci.*, 2018, **19**(5), E1461.

16 J. Xu, X. Liu, L. Luo, *et al.*, A Metabonomics Investigation into the Therapeutic Effects of BuChang NaoXinTong Capsules on Reversing the Amino Acid-Protein Interaction Network of Cerebral Ischemia, *Oxid. Med. Cell. Longevity*, 2019, **2019**, 7258624.

17 H. Zhu, Z. Wang, Y. Wu, *et al.*, Untargeted metabonomics reveals intervention effects of chicory polysaccharide in a rat model of non-alcoholic fatty liver disease, *Int. J. Biol. Macromol.*, 2019, **128**, 363–375.

18 A. Zhang, H. Sun, G. Yan, *et al.*, Metabolomics in diagnosis and biomarker discovery of colorectal cancer, *Cancer Lett.*, 2014, **345**(1), 17–20.
19 S. Qiu, A. Zhang, T. Zhang, *et al.*, Dissect new mechanistic insights for geniposide efficacy on the hepatoprotection using multiomics approach, *Oncotarget*, 2017, **8**(65), 108760–108770.
20 A. Zhang, H. Sun and X. Wang, Urinary metabolic profiling of rat models revealed protective function of scoparone against alcohol induced hepatotoxicity, *Sci. Rep.*, 2014, **4**, 6768.
21 X. Wang, X. Gao, A. Zhang, *et al.*, High-throughput metabolomics for evaluating the efficacy and discovering the metabolic mechanism of Luozhen capsules from the excessive liver-fire syndrome of hypertension, *RSC Adv.*, 2019, **9**(55), 32141–32153.
22 A. Zhang, Z. Ma, H. Sun, *et al.*, High-Throughput Metabolomics Evaluate the Efficacy of Total Lignans From Acanthophanax Senticosus Stem Against Ovariectomized Osteoporosis Rat, *Front. Pharmacol.*, 2019, **10**, 553.
23 A. Zhang, H. Sun, G. Yan, *et al.*, Mass spectrometry-based metabolomics: applications to biomarker and metabolic pathway research, *Biomed. Chromatogr.*, 2016, **30**(1), 7–12.
24 H. Dong, A. Zhang, H. Sun, *et al.*, Ingenuity pathways analysis of urine metabolomics phenotypes toxicity of Chuanwu in Wistar rats by UPLC-Q-TOF-HDMS coupled with pattern recognition methods, *Mol. BioSyst.*, 2012, **8**(4), 1206–1221.
25 A. Zhang, H. Sun, P. Wang, *et al.*, Modern analytical techniques in metabolomics analysis, *Analyst*, 2012, **137**(2), 293–300.
26 A. H. Zhang, J. B. Yu, H. Sun, *et al.*, Identifying quality-markers from Shengmai San protects against transgenic mouse model of Alzheimer's disease using chinmedomics approach, *Phytomedicine*, 2018, **45**, 84–92.
27 A. Zhang, H. Sun, H. Xu, *et al.*, Cell metabolomics, *OMICS: J. Integr. Biol.*, 2013, **17**(10), 495–501.
28 X. Wang, A. Zhang, X. Zhou, *et al.*, An integrated chinmedomics strategy for discovery of effective constituents from traditional herbal medicine, *Sci. Rep.*, 2016, **6**, 18997.
29 Y. F. Li, S. Qiu, L. J. Gao, *et al.*, Metabolomic estimation of the diagnosis of hepatocellular carcinoma based on ultrahigh performance liquid chromatography coupled with time-of-flight mass spectrometry, *RSC Adv.*, 2018, **8**(17), 9375–9382.
30 X. Wang, J. Li and A. H. Zhang, Urine metabolic phenotypes analysis of extrahepatic cholangiocarcinoma disease using ultra-high performance liquid chromatography-mass spectrometry, *RSC Adv.*, 2016, **6**(67), 63049–63057.
31 A. Zhang, H. Sun, G. Yan, *et al.*, Metabolomics study of type 2 diabetes using ultra-performance LC-ESI/quadrupole-TOF high-definition MS coupled with pattern recognition methods, *J. Physiol. Biochem.*, 2014, **70**(1), 117–128.
32 H. Wang, G. Yan, A. Zhang, *et al.*, Rapid discovery and global characterization of chemical constituents and rats metabolites of *Phellodendri amurensis* cortex by ultra-performance liquid chromatography-electrospray ionization/quadrupole-time-of-flight mass spectrometry coupled with pattern recognition approach, *Analyst*, 2013, **138**(11), 3303–3312.
33 A. Zhang, H. Sun, S. Qiu, *et al.*, Metabolomics insights into pathophysiological mechanisms of nephrology, *Int. Urol. Nephrol.*, 2014, **46**(5), 1025–1030.
34 H. Sun, A. H. Zhang, Q. Song, *et al.*, Functional metabolomics discover pentose and glucuronate interconversion pathways as promising targets for Yang Huang syndrome treatment with Yinchenhao Tang, *RSC Adv.*, 2018, **8**, 36831–36839.
35 Y. Zhao, H. Lv, S. Qiu, *et al.*, Plasma metabolic profiling and novel metabolite biomarkers for diagnosing prostate cancer, *RSC Adv.*, 2017, **7**(48), 30060–30069.
36 X. N. Li, A. Zhang, M. Wang, *et al.*, Screening the active compounds of *Phellodendri amurensis* cortex for treating prostate cancer by high-throughput chinmedomics, *Sci. Rep.*, 2017, **7**, 46234.
37 A. Zhang, H. Sun, Y. Han, *et al.*, Urinary metabolic biomarker and pathway study of hepatitis B virus infected patients based on UPLC-MS system, *PLoS One*, 2013, **8**(5), e64381.
38 H. Sun, A. Zhang and X. Wang, Potential role of metabolomic approaches for Chinese medicine syndromes and herbal medicine, *Phytother. Res.*, 2012, **26**(10), 1466–1471.
39 A. Zhang, H. Sun, P. Wang, *et al.*, Salivary proteomics in biomedical research, *Clin. Chim. Acta*, 2013, **415**, 261–265.
40 H. Fang, A. H. Zhang, H. Sun, *et al.*, High-throughput metabolomics screen coupled with multivariate statistical analysis identifies therapeutic targets in alcoholic liver disease rats using liquid chromatography-mass spectrometry, *J. Chromatogr. B: Anal. Technol. Biomed. Life Sci.*, 2019, **1109**, 112–120.
41 A. Zhang, H. Sun and X. Wang, Emerging role and recent applications of metabolomics biomarkers in obesity disease research, *RSC Adv.*, 2017, **7**(25), 14966–14973.
42 H. Xiong, A. H. Zhang, Q. Q. Zhao, *et al.*, Discovery and screening quality-marker ingredients of *Panax quinquefolius* using chinmedomics approach, *Phytomedicine*, 2019, 152928.
43 A. Zhang, H. Wang, H. Sun, *et al.*, Metabolomics strategy reveals therapeutical assessment of limonin on nonbacterial prostatitis, *Food Funct.*, 2015, **6**(11), 3540–3549.
44 H. L. Zhang, A. H. Zhang, X. H. Zhou, *et al.*, High-throughput lipidomics reveal mirabilite regulating lipid metabolism as anticancer therapeutics, *RSC Adv.*, 2018, **8**(62), 35600–35610.
45 H. Sun, A. Zhang, L. Yang, *et al.*, High-throughput chinmedomics strategy for discovering the quality-markers and potential targets for Yinchenhao decoction, *Phytomedicine*, 2019, **54**, 328–338.
46 H. Sun, A. Zhang, G. Yan, *et al.*, Metabolomic analysis of key regulatory metabolites in hepatitis C virus-infected tree shrews, *Mol. Cell. Proteomics*, 2013, **12**(3), 710–719.

47 A. Zhang, H. Sun and X. Wang, Potentiating therapeutic effects by enhancing synergism based on active constituents from traditional medicine, *Phytother. Res.*, 2014, **28**(4), 526–533.
48 Y. Nan, X. Zhou, Q. Liu, *et al.*, Serum metabolomics strategy for understanding pharmacological effects of ShenQi pill acting on kidney yang deficiency syndrome, *J. Chromatogr. B: Anal. Technol. Biomed. Life Sci.*, 2016, **1026**, 217–226.
49 J. Xie, A. H. Zhang and S. Qiu, Identification of the perturbed metabolic pathways associating with prostate cancer cells and anticancer affects of obacunone, *J. Proteomics*, 2019, **206**, 103447.
50 A. Zhang, H. Sun, P. Wang, *et al.*, Future perspectives of personalized medicine in traditional Chinese medicine: a systems biology approach, *Complement. Ther. Med.*, 2012, **20**(1–2), 93–99.
51 Y. Zhang, P. Liu, Y. Li, *et al.*, Exploration of metabolite signatures using high-throughput mass spectrometry coupled with multivariate data analysis, *RSC Adv.*, 2017, **7**, 6780–6787.
52 L. Wang, H. Dong, A. H. Zhang, *et al.*, Exploring the detoxification effects and mechanism of Caowu in prescription using liquid chromatography-high-resolution mass spectrometry-based metabolomics, *Open J. Proteom. Genom.*, 2018, **3**(1), 011–023.
53 A. H. Zhang, H. Sun, G. L. Yan, *et al.*, Chinmedomics: A Powerful Approach Integrating Metabolomics with Serum Pharmacochemistry to Evaluate the Efficacy of Traditional Chinese Medicine, *Engineering*, 2019, **5**, 60–68.
54 H. Sun, H. L. Zhang, A. H. Zhang, *et al.*, Network pharmacology combined with functional metabolomics discover bile acid metabolism as a promising target for mirabilite against colorectal cancer, *RSC Adv.*, 2018, **8**, 30061–30070.
55 Q. Liang, H. Liu, X. Li, *et al.*, High-throughput metabolomics analysis discovers salivary biomarkers for predicting mild cognitive impairment and Alzheimer's disease, *RSC Adv.*, 2016, **6**, 75499–75504.
56 X. J. Wang, J. L. Ren, A. H. Zhang, *et al.*, Novel applications of mass spectrometry-based metabolomics in herbal medicines and its active ingredients: Current evidence, *Mass Spectrom. Rev.*, 2019, **38**(4–5), 380–402.
57 H. Sun, A. H. Zhang, S. B. Liu, *et al.*, Cell metabolomics identify regulatory pathways and targets of magnoline against prostate cancer, *J. Chromatogr. B: Anal. Technol. Biomed. Life Sci.*, 2018, **1102–1103**, 143–151.
58 H. Zhang, A. Zhang, J. Miao, *et al.*, Targeting regulation of tryptophan metabolism for colorectal cancer therapy: a systematic review, *RSC Adv.*, 2019, **9**, 3072–3080.
59 A. Zhang, H. Sun, S. Qiu, *et al.*, NMR-based metabolomics coupled with pattern recognition methods in biomarker discovery and disease diagnosis, *Magn. Reson. Chem.*, 2013, **51**(9), 549–556.
60 C. C. Feng, A. H. Zhang, J. H. Miao, *et al.*, Recent advances in understanding cross-talk between Bile Acids and Gut Microbiota, *Open J. Proteom. Genom.*, 2018, **3**(1), 024–034.
61 H. Cao, A. Zhang, H. Zhang, *et al.*, The application of metabolomics in traditional Chinese medicine opens up a dialogue between Chinese and Western medicine, *Phytother. Res.*, 2015, **29**(2), 159–166.
62 X. Liu, A. Zhang, H. Fang, *et al.*, Serum metabolomics strategy for understanding the therapeutic effects of Yin-Chen-Hao-Tang against Yanghuang syndrome, *RSC Adv.*, 2018, **8**, 7403–7413.
63 A. Zhang, H. Sun, G. Yan, *et al.*, Metabolomics in diagnosis and biomarker discovery of colorectal cancer, *Cancer Lett.*, 2014, **345**(1), 17–20.
64 A. Zhang, H. Sun, Y. Han, *et al.*, Exploratory urinary metabolic biomarkers and pathways using UPLC-Q-TOF-HDMS coupled with pattern recognition approach, *Analyst*, 2012, **137**(18), 4200–4208.
65 X. Li, A. Zhang, H. Sun, *et al.*, Metabolic characterization and pathway analysis of berberine protects against prostate cancer, *Oncotarget*, 2017, **8**, 65022–65041.
66 H. Fang, A. Zhang, J. Yu, *et al.*, Insight into the metabolic mechanism of scoparone on biomarkers for inhibiting Yanghuang syndrome, *Sci. Rep.*, 2016, **6**, 37519.
67 A. Zhang, H. Sun, G. Yan, *et al.*, Mass spectrometry-based metabolomics: applications to biomarker and metabolic pathway research, *Biomed. Chromatogr.*, 2016, **30**(1), 7–12.
68 H. Chu, A. Zhang, Y. Han, *et al.*, Metabolomics approach to explore the effects of Kai-Xin-San on Alzheimer's disease using UPLC/ESI-Q-TOF mass spectrometry, *J. Chromatogr. B: Anal. Technol. Biomed. Life Sci.*, 2016, **1015**, 50–61.
69 A. Zhang, H. Sun, G. Yan, *et al.*, Metabolomics for biomarker discovery: moving to the clinic, *BioMed Res. Int.*, 2015, **2015**, 354671.
70 H. Sun, H. Wang, A. Zhang, *et al.*, Berberine ameliorates nonbacterial prostatitis *via* multi-target metabolic network regulation, *OMICS: J. Integr. Biol.*, 2015, **19**(3), 186–195.
71 A. Zhang, S. Qiu, H. Xu, *et al.*, Metabolomics in diabetes, *Clin. Chim. Acta*, 2014, **429**, 106–110.
72 H. Sun, X. Li, A. Zhang, *et al.*, Exploring potential biomarkers of coronary heart disease treated by Jing Zhi Guan Xin Pian using high-throughput metabolomics, *RSC Adv.*, 2019, **9**(20), 11420–11432.
73 A. Zhang, H. Sun, G. Yan, *et al.*, Serum proteomics in biomedical research: a systematic review, *Appl. Biochem. Biotechnol.*, 2013, **170**(4), 774–786.
74 X. Li, Y. Han, A. Zhang, *et al.*, Mechanistic and Therapeutic Advances in Colon Cancer: A Systematic Review, *Open J. Proteom. Genom.*, 2019, **4**(1), 001–012.
75 H. Sun, M. Wang, A. Zhang, *et al.*, UPLC-Q-TOF-HDMS Analysis of Constituents in the Root of Two Kinds of Aconitum Using a Metabolomics Approach, *Phytochem. Anal.*, 2013, **24**(3), 263–276.
76 A. Zhang, H. Sun and X. Wang, Potentiating therapeutic effects by enhancing synergism based on active constituents from traditional medicine, *Phytother. Res.*, 2014, **28**(4), 526–533.
77 G. Yan, A. Zhang, H. Sun, *et al.*, An effective method for determining the ingredients of Shuanghuanglian formula

in blood samples using high-resolution LC-MS coupled with background subtraction and a multiple data processing approach, *J. Sep. Sci.*, 2013, **36**(19), 3191–3199.

78 A. Zhang, H. Sun, S. Qiu, *et al.*, Metabolomics in noninvasive breast cancer, *Clin. Chim. Acta*, 2013, **424**, 3–7.

79 Q. Liang, Y. Zhu, H. Liu, *et al.*, High-throughput lipidomics enables discovery of the mode of action of huaxian capsule impacting the metabolism of sepsis, *RSC Adv.*, 2017, **7**(71), 44990–44996.

80 Y. Zhao, H. Lv, S. Qiu, *et al.*, Plasma metabolic profiling and novel metabolite biomarkers for diagnosing prostate cancer, *RSC Adv.*, 2017, **7**(48), 30060–30069.

81 Q. Liang, H. Liu, L. Xie, *et al.*, High-throughput and multi-dimensional omics approach uncovers a huaxian capsule to ameliorate the dysregulated expression profiling of severe sepsis rats, *RSC Adv.*, 2017, **7**(32), 19894–19903.

82 X. Wu, X. Sun, C. Zhao, *et al.*, Exploring the pharmacological effects and potential targets of paeoniflorin on the endometriosis of cold coagulation and blood stasis model rats by ultra-performance liquid chromatography tandem mass spectrometry with a pattern recognition approach, *RSC Adv.*, 2019, **9**(36), 20796–20805.

83 Q. Liang, H. Liu, Y. Jiang, *et al.*, Novel liquid chromatography-mass spectrometry for metabolite biomarkers of acute lung injury disease, *Anal. Methods*, 2016, **8**(31), 6017–6022.

84 Q. Liang, H. Liu, L. Xie, *et al.*, High-throughput metabolomics enables biomarker discovery in prostate cancer, *RSC Adv.*, 2017, **7**(5), 2587–2593.

85 A. Zhang, S. Qiu, H. Sun, T. Zhang, Y. Guan, Y. Han, G. Yan and X. Wang, Scoparone affects lipid metabolism in primary hepatocytes using lipidomics, *Sci. Rep.*, 2016, **6**, 28031.

86 Q. Liang, H. Liu, X. Li, *et al.*, High-throughput metabolomics analysis discovers salivary biomarkers for predicting mild cognitive impairment and Alzheimer's disease, *RSC Adv.*, 2016, **6**(79), 75499–75504.

87 Q. Liang, H. Liu, H. Xing, *et al.*, UPLC-QTOF/MS based metabolomics reveals metabolic alterations associated with severe sepsis, *RSC Adv.*, 2016, **6**, 43293–43298.

88 Y. Li, S. Qiu and A. Zhang, High-throughput metabolomics to identify metabolites serve as diagnostic biomarkers of prostate cancer, *Anal. Methods*, 2016, **8**, 3284–3290.

89 Q. Liang, H. Liu, H. Xing, *et al.*, High-resolution mass spectrometry for exploring metabolic signatures of sepsis-induced acute kidney injury, *RSC Adv.*, 2016, **6**, 29863–29868.

90 Q. Liang, H. Liu, H. Xing, *et al.*, Urinary UPLC-MS metabolomics dissecting the underlying mechanisms of huaxian capsule protects against sepsis, *RSC Adv.*, 2016, **6**, 40436–40441.

91 Q. Liang, H. Liu, Y. Jiang, *et al.*, High-throughput metabolic profiling for discovering metabolic biomarkers of sepsis-induced acute lung injury, *RSC Adv.*, 2016, **6**, 11008–11013.

92 Q. Liang, H. Liu, T. Zhang, *et al.*, Untargeted lipidomics study of coronary artery disease by FUPLC-Q-TOF-MS, *Anal. Methods*, 2016, **8**(6), 1229–1234.

93 Q. Liang, H. Liu, Y. Jiang, *et al.*, Discovering lipid phenotypic changes of sepsis-induced lung injury using high-throughput lipidomic analysis, *RSC Adv.*, 2016, **6**, 38233–38237.

94 Q. Liang, H. Liu, T. Zhang, *et al.*, Discovery of serum metabolites for diagnosis of mild cognitive impairment to Alzheimer's disease progression using an optimized metabolomics method, *RSC Adv.*, 2016, **6**, 3586–3591.

95 A. Zhang, G. Yan, H. Sun, *et al.*, Deciphering the biological effects of acupuncture treatment modulating multiple metabolism pathways, *Sci. Rep.*, 2016, **6**, 19942.

96 Q. Liang, H. Liu, T. Zhang, *et al.*, Metabolomics-Based Screening of Salivary Biomarkers for Early Diagnosis of Alzheimer's Disease, *RSC Adv.*, 2015, **5**, 96074–96079.

97 Q. Liang, H. Liu, T. Zhang, *et al.*, Potential urine biomarkers from a high throughput metabolomics study of severe sepsis in a large Asian cohort, *RSC Adv.*, 2015, **5**, 102204–102209.

98 Q. Liang, C. Wang, B. Li, *et al.*, Metabolomics of Alcoholic Liver Disease: A Clinical Discovery Study, *RSC Adv.*, 2015, **5**, 80381–80387.

99 Q. Liang, C. Wang, B. Li, *et al.*, Lipidomics Analysis Based on Liquid Chromatography Mass Spectrometry for Hepatocellular Carcinoma and Intrahepatic Cholangiocarcinoma, *RSC Adv.*, 2015, **5**, 63711–63718.

100 Q. Liang, C. Wang, B. Li, *et al.*, Metabolic footprinting to understand therapeutic effects and mechanisms of silybin on acute liver damage in rat, *Pharmacogn. Mag.*, 2015, **11**(43), 586–593.

123 D. Techer, S. Milla, P. Fontaine, *et al.*, Influence of waterborne gallic and pelargonic acid exposures on biochemical and reproductive parameters in the zebrafish (*Danio rerio*), *Environ. Toxicol.*, 2017, **32**(1), 227–240.

124 R. M. Heuer and M. Grosell, Physiological impacts of elevated carbon dioxide and ocean acidification on fish, *Am. J. Physiol.: Regul., Integr. Comp. Physiol.*, 2014, **307**(9), R1061–R1084.

125 R. Ern and A. J. Esbaugh, Effects of salinity and hypoxia-induced hyperventilation on oxygen consumption and cost of osmoregulation in the estuarine red drum (*Sciaenops ocellatus*), *Comp. Biochem. Physiol., Part A: Mol. Integr. Physiol.*, 2018, **08**, 22252–22259.

126 S. M. Cao, Y. Y. Wu, L. H. Li, *et al.*, Activities of Endogenous Lipase and Lipolysis Oxidation of Low-Salt Lactic Acid-Fermented Fish (*Decapterus maruadsi*), *J. Oleo Sci.*, 2018, **67**(4), 445–453.

127 P. A. Wright, C. M. Wood, J. Hiroi, *et al.*, (Uncommon) Mechanisms of Branchial Ammonia Excretion in the Common Carp (*Cyprinus carpio*) in Response to Environmentally Induced Metabolic Acidosis, *Physiol. Biochem. Zool.*, 2016, **89**(1), 26–40.

128 S. F. Chew and Y. K. Ip, Excretory nitrogen metabolism and defence against ammonia toxicity in air-breathing fishes, *J. Fish Biol.*, 2014, **84**(3), 603–638.

129 A. M. Loong, Y. R. Chng, S. F. Chew, *et al.*, Molecular characterization and mRNA expression of carbamoyl phosphate synthetase III in the liver of the African lungfish, *Protopterus annectens*, during aestivation or exposure to ammonia, *J. Comp. Physiol., B*, 2012, **182**(3), 367–379.

130 P. Wang, H. Sun, H. Lv, *et al.*, Thyroxine and reserpine-induced changes in metabolic profiles of rat urine and the therapeutic effect of Liu Wei Di Huang Wan detected by UPLC-HDMS, *J. Pharm. Biomed. Anal.*, 2010, **53**(3), 631–645.

131 X. Wang, H. Sun, A. Zhang, *et al.*, Ultra-performance liquid chromatography coupled to mass spectrometry as a sensitive and powerful technology for metabolomic studies, *J. Sep. Sci.*, 2011, **34**(24), 3451–3459.

132 B. Yang, W. Dong, A. Zhang, *et al.*, Ultra-performance liquid chromatography coupled with electrospray ionization/quadrupole-time-of-flight mass spectrometry for rapid analysis of constituents of Suanzaoren decoction, *J. Sep. Sci.*, 2011, **34**(22), 3208–3215.

133 X. Wang, H. Sun, A. Zhang, *et al.*, Potential role of metabolomics apporoaches in the area of traditional Chinese medicine: as pillars of the bridge between Chinese and Western medicine, *J. Pharm. Biomed. Anal.*, 2011, **55**(5), 859–868.

134 W. Dong, P. Wang, X. Meng, *et al.*, Ultra-performance liquid chromatography-high-definition mass spectrometry analysis of constituents in the root of Radix Stemonae and those absorbed in blood after oral administration of the extract of the crude drug, *Phytochem. Anal.*, 2012, **23**(6), 657–667.

135 A. Zhang, H. Sun, Z. Wang, *et al.*, Metabolomics: towards understanding traditional Chinese medicine, *Planta Med.*, 2010, **76**(17), 2026–2035.

136 B. Yang, A. Zhang, H. Sun, *et al.*, Metabolomic study of insomnia and intervention effects of Suanzaoren decoction using ultra-performance liquid-chromatography/electrospray-ionization synapt high-definition mass spectrometry, *J. Pharm. Biomed. Anal.*, 2012, **58**, 113–124.

137 H. Sun, Y. Han, A. Zhang, X. Meng, *et al.*, UPLC-MS based metabolic profiling of the phenotypes of *Acanthopanax senticosus* reveals the changes in active metabolites distinguishing the diversities of the plant grown in northeast area of China, *Chin. J. Nat. Med.*, 2012, **10**(3), 196–206.

138 A. Zhang, H. Sun, P. Wang, *et al.*, Metabonomics for discovering biomarkers of hepatotoxicity and nephrotoxicity, *Pharmazie*, 2012, **67**(2), 99–105.

139 X. Wang, B. Yang, A. Zhang, *et al.*, Potential drug targets on insomnia and intervention effects of Jujuboside A through metabolic pathway analysis as revealed by UPLC/ESI-SYNAPT-HDMS coupled with pattern recognition approach, *J. Proteomics*, 2012, **75**(4), 1411–1427.

140 A. Zhang, H. Sun and X. Wang, Saliva metabolomics opens door to biomarker discovery, disease diagnosis, and treatment, *Appl. Biochem. Biotechnol.*, 2012, **168**(6), 1718–1727.

141 H. Sun, W. Dong, A. Zhang, *et al.*, Ultra-performance liquid-chromatography with tandem mass spectrometry performing pharmacokinetic and biodistribution studies of croomine, neotuberostemonine and tuberostemonine alkaloids absorbed in the rat plasma after oral administration of Stemonae Radix, *Fitoterapia*, 2012, **83**(8), 1699–1705.

142 A. Zhang, H. Sun, X. Wu, *et al.*, Urine metabolomics, *Clin. Chim. Acta*, 2012, **414**, 65–69.

143 H. Sun, W. Dong, A. Zhang, *et al.*, Pharmacokinetics study of multiple components absorbed in rat plasma after oral administration of Stemonae radix using ultra-performance liquid-chromatography/mass spectrometry with automated MetaboLynx software analysis, *J. Sep. Sci.*, 2012, **35**(24), 3477–3485.

144 X. Wang, A. Zhang and H. Sun, Future perspectives of Chinese medical formulae: chinmedomics as an effector, *OMICS: J. Integr. Biol.*, 2012, **16**(7–8), 414–421.

145 X. Wang, A. Zhang, H. Sun, *et al.*, Network generation enhances interpretation of proteomics data sets by a combination of two-dimensional polyacrylamide gel electrophoresis and matrix-assisted laser desorption/ionization-time of flight mass spectrometry, *Analyst*, 2012, **137**(20), 4703–4711.

146 H. Sun, B. Ni, A. Zhang, *et al.*, Metabolomics study on Fuzi and its processed products using ultra-performance liquid-chromatography/electrospray-ionization synapt high-definition mass spectrometry coupled with pattern recognition analysis, *Analyst*, 2012, **137**(1), 170–185.

147 A. Zhang, H. Sun, P. Wang, *et al.*, Recent and potential developments of biofluid analyses in metabolomics, *J. Proteomics*, 2012, **75**(4), 1079–1088.

148 X. Wang, H. Wang, A. Zhang, *et al.*, Metabolomics study on the toxicity of aconite root and its processed products using ultraperformance liquid-chromatography/electrospray-ionization synapt high-definition mass spectrometry coupled with pattern recognition approach and ingenuity pathways analysis, *J. Proteome Res.*, 2012, **11**(2), 1284–1301.

149 X. Wang, B. Yang, H. Sun, *et al.*, Pattern recognition approaches and computational systems tools for ultra performance liquid chromatography-mass spectrometry-based comprehensive metabolomic profiling and pathways analysis of biological data sets, *Anal. Chem.*, 2012, **84**(1), 428–439.

150 M. Oner, G. Atli and M. Canli, Changes in serum biochemical parameters of freshwater fish *Oreochromis niloticus* following prolonged metal (Ag, Cd, Cr, Cu, Zn) exposures, *Environ. Toxicol. Chem.*, 2008, **27**(2), 360–366.

151 L. Wang, S. M. Harris, H. M. Espinoza, *et al.*, Characterization of phospholipid hydroperoxide glutathione metabolizing peroxidase (gpx4) isoforms in Coho salmon olfactory and liver tissues and their modulation by cadmium, *Aquat. Toxicol.*, 2012, **114–115**, 134–141.

152 P. L. P. F. Carvalho, F. Y. Yamamoto, M. M. Barros, *et al.*, L-Glutamine *in vitro* supplementation enhances Nile tilapia *Oreochromis niloticus* (Linnaeus, 1758) leukocyte function, *Fish Shellfish Immunol.*, 2018, 80592–80599.

153 A. K. Dhanasiri, J. M. Fernandes and V. Kiron, Glutamine synthetase activity and the expression of three glul paralogues in zebrafish during transport, *Comp. Biochem. Physiol., Part B: Biochem. Mol. Biol.*, 2012, **163**(3–4), 274–284.

154 Q. Yan, S. Xie, X. Zhu, *et al.*, Dietary methionine requirement for juvenile rockfish, *Sebastes schlegelii*, *Aquacult. Nutr.*, 2010, **13**(3), 163–169.

155 J. P. Wang, J. S. Yoo, H. J. Kim, *et al.*, Nutrient digestibility blood profiles and fecal microbiota are influenced by chitooligosaccharide supplementation of growing pigs, *Livest. Prod. Sci.*, 2009, **125**(2), 298–303.

156 J. Balakrishnan, S. Dhavamani, S. G. Sadasivam, *et al.*, Omega-3-rich Isochrysis sp. biomass enhances brain docosahexaenoic acid levels and improves serum lipid profile and antioxidant status in Wistar rats, *J. Sci. Food Agric.*, 2019, **99**(13), 6066–6075.

157 S. Kumar, N. P. Sahu, A. K. Pal, *et al.*, Effect of dietary carbohydrate on haematology, respiratory burst activity and histological changes in Lrohita juveniles, *Fish Shellfish Immunol.*, 2005, **19**(4), 331–344.

158 N. T. Frick and P. A. Wright, Nitrogen metabolism and excretion in the mangrove killifish *Rivulus marmoratus* II. Significant ammonia volatilization in a teleost during air-exposure, *J. Exp. Biol.*, 2002, **205**, 91–100.

159 N. Kumar, K. K. Krishnani and N. P. Singh, Oxidative and Cellular Metabolic Stress of Fish: An Appealing Tool for Biomonitoring of Metal Contamination in the Kolkata Wetland, a Ramsar Site, *Arch. Environ. Contam. Toxicol.*, 2019, **76**(3), 469–482.

160 W. N. Wang, A. L. Wang, L. Chen, *et al.*, Effects of pH on survival, phosphorus concentration, adenylate energy charge and Na + -K + ATPase activities of *Penaeus chinensis* Osbeck juveniles, *Aquat. Toxicol.*, 2002, **60**, 75–83.

161 J. H. Kim and J. C. Kang, The arsenic accumulation and its effect on oxidative stress responses in juvenile rockfish, *Sebastes schlegelii*, exposed to waterborne arsenic (As^{3+}), *Environ. Toxicol. Pharmacol.*, 2015, **39**(2), 668.